Umberto A. Maccarone

HEAVY MINERALS IN EXPERIMENTAL TURBIDITES

Umberto A. Maccarone; Heavy mineral behaviour in experimentally produced turbidite beds; Department of Geological Sciences; Degree of Master of Science.

ABSTRACT

Sulfide deposits have been recognized in nature within turbidites.

In the present flume experiments, ilmenite and silica were mainly used as sediments. Densities of over 2 were obtained. A linear relation exists between velocity and density of the initial flow.

Where the turbidites tapered off markedly downflume, the following phenomena were noted:

(1) Low density runs formed the richest concentrations of dense mineral;

(2) Slurries in which the sediments were difficult to keep in suspension were impoverished in heavy minerals in the turbidite. Most of the load slumped and showed lateral and vertical grading in particle sizes and in per cent of heavy minerals.

Coarser material in the initial flow will decrease the velocity of the turbidity current as well as decrease the Froude and Reynold's numbers.

The results of these turbidity current experiments are compared to natural sulfide-bearing turbidites reported in the literature.

Umberto A. Maccarone; Heavy mineral behaviour in experimentally produced turbidite beds; Department of Geological Sciences; Degree of Master of Science.

SOMMAIRE

Des gisements de sulfures se retrouvent au sein de turbidites dans la nature.

Surtout l'ilménite et la silice agissaient comme sédiments dans cette étude. Des densités de deux (2.0) et au-delà furent atteintes. La vitesse augmentait parallèlement avec la densité initiale.

Deux séries de données furent mises en évidence lorsque l'épaisseur des dépôts diminuait rapidement dans le sens du courant:

(1) La plus grande concentration de minéraux fut retrouvée dans les écoulements de faibles densités;

(2) Les sédiments qui ne se maintenaient en suspension qu'avec difficulté formaient des turbidites déficientes en minéraux lourds. Ces derniers s'affaisaient pour la plupart en amont du réservoir et accusaient un granoclassement. Le pourcentage des minéraux lourds varie comme le granoclassement.

L'emploi de grains plus grossiers diminue la vitesse du courant ainsi que les nombres de Reynold et de Froude.

Les résultats expérimentaux sont utilisés pour expliquer les turbidites minéralisées en sulfures.

HEAVY MINERAL BEHAVIOUR IN EXPERIMENTALLY PRODUCED TURBIDITE BEDS

by

Umberto Antonio Maccarone

A Thesis Submitted to the Faculty of Graduate Studies and Research of McGill University in Partial Fulfillment of the Requirements for the Degree of Master of Science in Geology

Montreal, Quebec

Canada

1972

TABLE OF CONTENTS

Chapter Page

LIST OF TABLES

LIST OF ILLUSTRATIONS

LIST OF PLATES

CHAPTER I

Introduction

The purpose of this thesis is to investigate the behaviour of heavy minerals carried within a turbidity current. The intention was not primarily to demonstrate the possibility of forming ore concentrations of minerals but rather to investigate heavy mineral behaviour in experimentally produced turbidite beds. Where ore concentration occurs, the fact will be stressed because of interest to the economic geologist. Although a fair number of experiments have been done on small-scale turbidity currents, this seems to be the first attempt to simulate sulfide enrichment through turbidity currents.

The thesis topic was suggested to me by Dr. L.A. Clark who had observed structures in Kuroko ore deposits in Japan which appeared to have been produced by turbidity currents.

Sulfide-laden turbidites have been recognized elsewhere in nature. Amstutz and Bubenicek (1967) describe primary depositional features in layered Pb-Cu-Ni-Co sulfide-bearing samples from the Upper Cambrian graywacke at Fredericktown, Missouri. Although the term 'turbidity current' is not explicitly mentioned as an agent of dense mineral transport and redistribution it is considered that the graded character of most graywackes is indicative of submarine generated turbidity flows (Pettijohn, 1957). This does not preclude other rock types of confirming a turbidite. However special attention will be paid in this paper to mineral deposits

which occur in graywacke. Garlick (1967) specifies that the typical host rocks of the stratiform Cu-Co-Fe sulfide ore deposits of Mufulira, Zambia are 'mottled quartzites and graywackes' formed by slumping and turbidity currents. He concludes that syngenetic chemical precipitation is largely responsible for the stratiform disseminated orebodies. Skinner (1958) suggested the redeposition of hydrous iron sulfide by turbidity currents in the formation of the pyrite and pyrrhotite-bearing graywackes and siltstones of the Nairne Pyritic Formation (Cambrian) in South Australia.

In this thesis data is presented on scaled experiments of turbidity currents in flumes in which the suspended material is quartz and ilmenite. This data is used to discuss the role of heavy minerals in natural turbidites.

Before describing experiments on turbidity currents we shall look more closely at the term 'turbidite'.

CHAPTER II

Turbidity Currents

A density or gravity current can be considered as a wedge of heavy fluid such as muddy water or cold air intruding into an expanse of lighter fluid such as clear water or warm air (Benjamin, 1968), because of differences in temperature or in concentration of solutes or suspended particles. In the present context a turbidity current will be considered as an underflow in a body of water, caused by a load of particles in suspension (Menard, 1964, p. 191) and (Middleton and Briggs, 1965).

Some turbidity currents can maintain themselves and transport sand and silt in turbulent suspension for distances of many hundreds of miles over a very gently sloping ocean bed (Bagnold, 1962). "Autosuspension" is a term used by Bagnold to refer to the spontaneous suspension of sediment in conditions of turbulent flow. The flow is partially maintained by the excess weight of the suspension relative to the ambient fluid (Middleton, 1966c). There is uncertainty concerning the ability of turbidity currents to achieve uniform flow while carrying coarse sediments. Middleton (1966b) doubts whether autosuspensions of sediment coarser than very fine sand can take place in nature.

Experimenters such as Kuenen and Middleton use the hydrostatic head of a suspension at the beginning of their flume to supply the driving force of the turbidity current. The interface between the denser, d1, and lighter

fluid, d2, in figure 1 shows a 'head wave' behind which there is a turbulent zone marked by eddies. Further back the interface becomes approximately parallel to the bed floor. The deposited sediments are referred to as a turbidite.

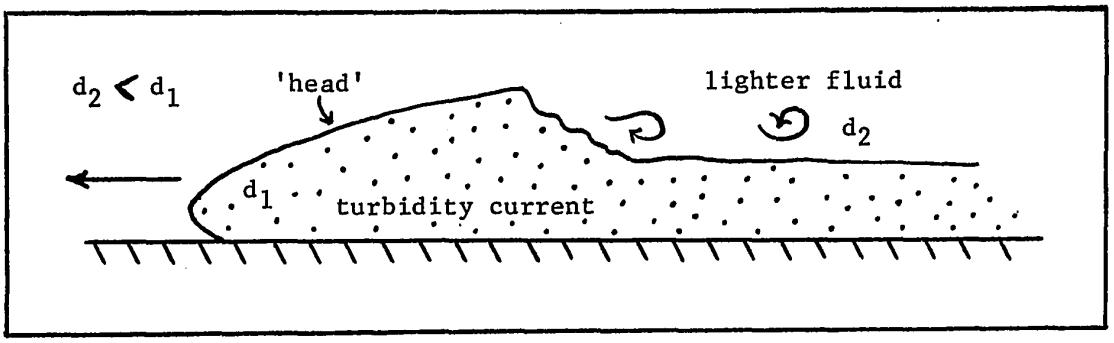

Figure 1. Observed form of turbidity current (modified after Benjamin (1968), and Keulegan (1958).

Evidence for the existence of submarine turbidity currents is found in:

1) The morphology of the continental slope.

Submarine canyons cross the continental slope to depths of several kilometers. Emery (1969, p. 116) believes that most of the evidence for the excavation of such canyons favors turbidity currents: "currents that arise when sediment slips down a slope and becomes mixed with overlying water, thereby increasing its density so that it continued down the slope often at high speed." At the lower end of the continental slope, large dejection cones join the submarine canyons to the abyssal plains. The dejection cones, or fans, represent in part the deposited load of turbidity currents (Nesteroff, 1965).

2) The sedimentary structures and the composition of piston cores taken from the fans and abyssal plains. These cores show, in places, sections of continental sands and littoral bioclastic sediments. The grains in single beds are graded vertically from coarse at the bottom to clays at the top and occur in a rhythmic fashion. These are defined as turbidites (Kuenen, 1957). The velocity of the current is high and the deposition of the sediment is rapid as evidenced by the aragonite tests of Pteropods and by pelagic foraminifera. Aragonite tests of Pteropods are not found in normally deposited muds below water depths of 2000 meters because they are thought to be dissolved rapidly when exposed to seawater at this depth. But Pteropod beds are found in turbidites at depths of 4000 meters in most abyssal plains; thus they must have been brought in and deposited rapidly. Similarly, the foraminifera Globigerina, found in turbidites at 6000 meters water depth, would normally have been dissolved by extended contact with seawater at this depth.

3) Submarine cable breaks.

Some submarine telegraph cable breaks are attributed to turbidity currents. Cable breaks occur successively downslope over a distance of several hundred kilometers in an interval of a few hours. Such breaks are well documented off the Grand Banks of Newfoundland, off Orleansville in Algeria and off Fiji (Menard, 1964; Ottman, 1965).

Flyschs and turbidites.

Many authors have noted the numerous common characteristics between modern turbidites and flysch sediments and have concluded that they were formed by turbidity currents. The Flysch corresponds roughly to the geosynclinal graywacke facies.

The composition of graywacke for the Hartz area and for the East Slovakian flysch was given by Dzulinski and Walton (1965) and is reproduced below:

Hartz area:	mean %	range %		mean %	range %
minerals			rocks		
quartz	40	25-53	igneous	10	4-16
plagioclase	31	20-42	sedimentary	5	2-7
feldspars	3	2-6	metamorphic	16	6-21
biotite	5	1-10	rock fragments	31	10-55
muscovite	3	1-7			
chlorite	14	4-17			
carbonate	2	0-6			
accessories	2	1-3			
free minerals	69	45-90			

East Slovakian flysch:

	mean %	range %
quartz and stable fragments	46	14-72
feldspar and unstable fragments	07	0-49
carbonate (cement)	23	0-71
matrix (clay)	22	0-47

The grain size of the particles in natural turbidites range from clay size up to 2 mm. When Shepard (1965) analysed 61 core samples of deep water turbidites he obtained a median particle diameter value of 0.180 mm. Almost all the sands were fine to very fine.

Bouma (in Jackson, 1970) subdivided the turbidite into five divisions:

e) Pelitic division
d) Upper division of parallel lamination
c) Division of current ripple lamination
b) Lower division of parallel lamination
a) Graded division.

Of Walker's (Walker, 1970, p. 228) analysis of 16,000 turbidite measurements, only 0.5 per cent did not conform with Bouma's sequence. This 0.5 per cent displayed minor reversals within the sequence. Walker finds that the topmost divisions e and d are usually not distinguishable, especially in older rocks, and considers Bouma's model in two parts. The main sandy and silty deposits are represented by divisions a, b and c, whereas the fines which are partly of turbidity current origin and partly of pelagic origin are shown by the d and e divisions.

Bouma's divisions do not apply well to carbonate rocks and modifications have been proposed (Walker, 1970).

CHAPTER III

Previous Work and Theory

INTRODUCTION

Many flume experiments have been performed to elucidate the dynamics of stream transport (Guy, Simons and Richardson, 1966). Fewer experiments have been done to study turbidity currents and no known experiments have been done on turbidity currents as agents of redistribution of heavy ore minerals.

The purpose of this chapter is to survey briefly some of the experimental work done on turbidity currents.

A. EXPERIMENTAL CONDITIONS

1. Flume Dimensions

The flumes range from 152.4 cm long x 25.4 cm deep x 5.7 cm wide (Bell 1942) to at least 1,030 cm long x 50 cm high x 15 cm wide (Kuenen and Menard, 1952).

2. Nature of the Particles

The types of sediments used in the experiments and of those found in nature are listed in table 1.

Table 1

Nature of Sediments in Turbidites

Authors	Sediments	
Bell, 1942	sand, sugar, salts	in experiments
Kuenen and Migliorini, 1950 Stong, 1963.	clay, sand, fine gravel, dilute sirup	
Dzulinski and Walton, 1965	plaster of Paris, charcoal dust	
Middleton, 1967	plastic beads	
Skinner, 1958	fine-grained graywackes and siltstones, sulfides	in nature
Garlick, 1967	graywackes with pebbles, arenite, sulfides	
Menard, 1969	graywackes and cherts	
van Andel and Komar, 1969	sand, gravel, calcareous oozes	

3. Concentration of the Flows

Middleton (1965, 1967) found that the mechanism of deposition and the type of graded bed deposited were different at a volume concentration (1 volume of sediment per unit volume of suspension) of about 30%. Consequently, he used two volume concentrations; about 23% and about 44% which correspond to average suspension densities of 1.12 and 1.22 respectively.

Kuenen (1950) worked with densities up to 2.0 by increasing the proportion of clay at the expense of sand. The largest grains may behave

as though they were suspended in a fluid whose density and viscosity is effectively that of the suspension of smaller grains. The effective settling velocity of the particles is reduced by the presence of the fine clays and also by high concentrations of sediment in the suspension (Middleton, 1966c, p. 205). This would permit high density currents to be formed.

Komar (1970, p. 1558, after Bagnold) suggests that the maximum densities attained by turbidity currents, in nature, over normal slopes do not exceed 1.18 g/cm^3 which corresponds to a volume concentration of 9 per cent. However, slightly greater densities may be reached in turbidity currents carrying dense minerals such as pyrite and pyrrhotite.

B. TURBIDITY CURRENT FLOW

1. The Start of the Flow

A semi-catastrophic event such as an earthquake or a submarine volcanic eruption may cause the initiation of a turbidity current. But not all modern or ancient turbidites are necessarily associated with volcanic events.

The hypothesis of an hydraulic jump expounded by van Andel and Komar (1969), after a model calculation of a turbidity current occurring in a basin, explains how a turbidity flow can start at the base of the initial slope. They wrote that "This jump converts a thin, high-speed, dense flow, essentially a slump or a slide, into a thick, low-density turbidity current and provides the energy for the dispersal of the material" (p. 1188).

Submarine slumping of water-saturated unconsolidated sediments on a

gentle slope, which give rise to turbidity currents further downslope, can also be triggered by abnormally long-wavelength storm waves (Jackson, 1970).

2. Velocity and Flow

Several velocity parameters are used in hydrodynamics. The settling or fall velocity (w) is the maximum rate of free fall of a particle in a fluid. The average velocity ($\bar{u}$) of a stream is the velocity averaged over a cross section normal to the direction of flow. The friction velocity or shear velocity (U_*) is defined as the square root of the tractive force (τ_o) divided by the density of the fluid (ρ): $U_* = \sqrt{\tau_o/\rho}$ (1)
It may be regarded as a measure of velocity near the bed.

Velocities of experimental turbidity currents flows range from a few centimeters per second up to about one meter per second. If the fluid particles move along smooth paths, the flow is said to be 'laminar'. Briggs and Middleton (1965) note that when the velocity or depth is large or if the kinematic viscosity of the fluid is very low, this type of flow breaks down and the fluid moves in a series of irregular eddies: the flow is now said to be 'turbulent'. There is now bulk diffusion of liquid and exchange of momentum between adjacent layers, and the velocity and shear constantly fluctuate about a mean value. The dynamic viscosity, μ, of a fluid is defined by Newton's Law of viscosity for a laminar flow:

$$\tau = \mu \, du/dy \qquad (2)$$

where τ is the shearing stress and du/dy is the rate of change of velocity normal to the direction of flow. The ratio, ν (nu) where $\nu = \frac{\mu}{\rho}$, is the kinematic viscosity. For turbulent flow, Newton's law is corrected

by the introduction of the coefficient of eddy viscosity (η):

$$\bar{\tau} = (\mu + \eta)\, d\bar{U}/dy \qquad (3)$$

where $\bar{\tau}$ is the average shear stress and $\frac{d\bar{U}}{dy}$, the average rate of shear.

The Reynolds Number is a dimensionless number which is proportional to the ratio between inertial and viscous forces. Commonly written as

$$Re = uL\rho/\mu \qquad (4)$$

and also as $$Re = 4\, u\, R/\nu \qquad (5)$$

where 'u' is the average velocity of the fluid, ρ is the density of the fluid, μ is the dynamic viscosity of the fluid, ν is the kinematic viscosity of the fluid, L is some appropriate measure of length and R the hydraulic radius. In this thesis R is taken as a measure of length. The hydraulic radius (R) is the area of the section of fluid normal to the average direction of flow, divided by the 'wetted perimeter':

$$R = w\, d/\, (w+2d) \qquad (6)$$

where 'w' is the width of the channel and 'd' is the depth of the uniform underflow.

A small Reynolds Number indicates the preponderance of viscous effects over inertial effect. The transition from 'laminar' to 'turbulent' flow takes place at a critical value of Reynolds Number (or range of numbers). For open straight channels this value is about 500 (Middleton and Briggs, 1965). A large Reynolds Number indicates the opposite.

Another dimensionless number which characterizes the type of flow is the Froude Number, Fr. For turbidity current,

$$Fr = \frac{u}{\sqrt{\frac{\Delta\rho}{\rho_t} \times g \times d}} \qquad (7)$$

where 'u' is the average velocity of the turbidity current, $\Delta\rho$ is the difference in density between the turbidity current (ρ_t) and the ambient fluid, 'g' is the acceleration due to gravity and 'd' is a characteristic length, usually the depth of flow (Menard, 1964) and (Middleton, 1966c). A critical value of the Froude Number (Fr = 1) may be used to distinguish two types of flow in open channels. For Fr < 1 (at low velocities or large depths) the flow is 'tranquil' and for Fr > 1 (at high velocities or small depths) the flow is 'rapid'. Middleton and Briggs (1965) stress an important distinction between the two types of flow: in tranquil flow, surface waves may be transmitted upstream, but in rapid flow the velocity of the fluid exceeds the velocity of propagation of long surface waves and it is impossible for such waves to move upstream. The larger the value of Fr, the larger is the inertial reaction to any force; the smaller the value of Fr, the larger is the role played by gravitational forces. A fixed numerical value of Fr then corresponds to a fixed coefficient of discharge, regardless of boundary scale. The Froude Number, therefore, is a similarity parameter for flow with gravitational acceleration. Model studies of flow with a free surface are invariably based on the Froude criterion of similitude.

The channel bottom has a certain drag effect on the fluid: the region where the bottom drag is felt is known as the 'boundary layer'. It includes a very thin layer close to the boundary which has a laminar flow, called 'laminar sublayer'. Fig. 2 depicts the conditions at the bed at the beginning of sediment movement.

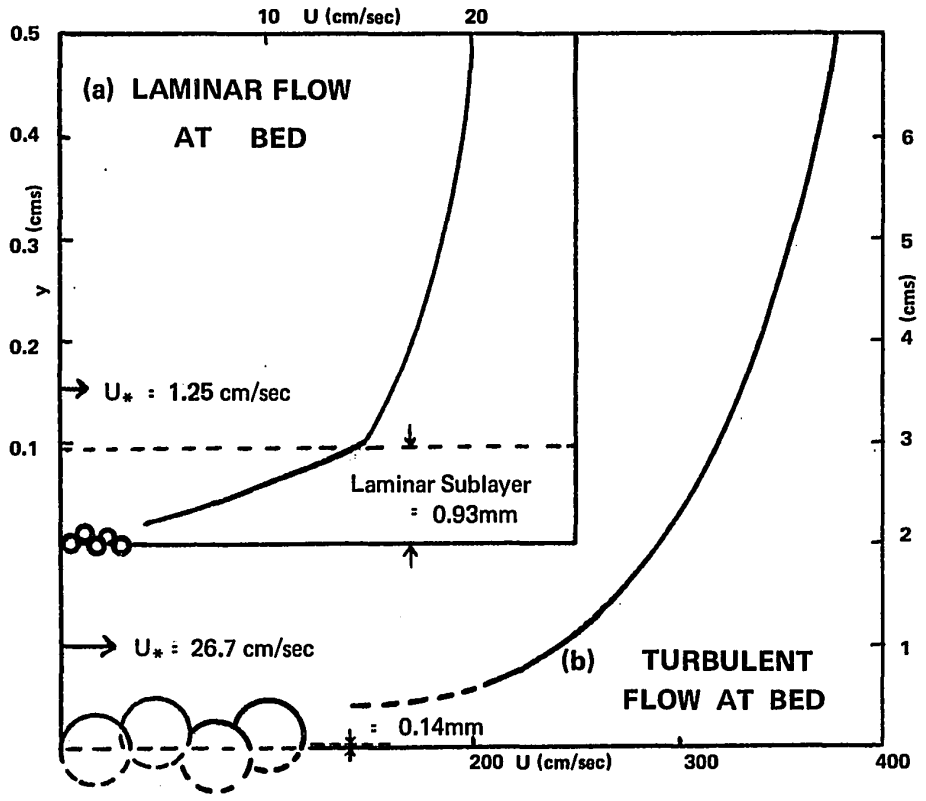

Figure 2. Conditions at the bed at the beginning of sediment movement, for two extreme conditions: (a) laminar flow at bed (smooth bed: grain diameter = 0.16 mm), (b) turbulence at bed (rough bed: grain diameter = 7.2 mm). The diagram shows that for laminar flow at the bed ($R_e = U_* d/\nu = 2$) the grains are fully enclosed in a laminar sublayer, whereas for turbulent flow at the bed ($R_e = 600$) the laminar sublayer is of negligible thickness compared with the size of the grains. (from figure 7 in Briggs and Middleton, 1965).

---

1. Where,

Re: the boundary Reynold's Number.

U_*: shear velocity, represents the velocity near the bed of a stream.

d : a measure of the height of the roughness elements of the boundary (e.g., the grain size of the sediments, for flat beds).

y : centimeters of the flow above the bottom.

ν : kinematic viscosity.

Estimates by various authors on the velocity of the turbidite currents on the Grand Banks in 1929 vary from 10 to 30 meters per second. Using the timing of the cable breaks Heezen and Ewing (1952) calculated a value of 30 meters per second for the initial velocity of the turbidity current on the continental slope. It subsequently decreased to 11 meters per second further down slope and on the continental rise. Kuenen (1952) obtained a value of 23.1 meters per second, assuming a broad flow advancing with a smooth front.

A detailed bathymetric chart and a physiographic diagram published after the articles of Heezen and Kuenen show that the breaks did not occur in a bowl-shaped valley as they had assumed but in a region containing fans and channels grading into an abyssal plain (Menard, 1964). Menard concludes that regardless of the path of the turbidity current, the speed reached 19.1 meters per second on the continental rise before decelerating to about 9.8 meters per second on the continental plain.

Komar (1970) calculated a velocity of 6.9 meters per second from his analyses of the dimensions and morphology of the Monterey deep-sea fan channel.

Using different roughness factors for the Cascadia deep-sea channel and different densities for the turbidity current flows, Hurley (1964) estimates the velocity as varying from 1 to 18.8 meters per second.

To predict the velocity of a turbidity current which has a uniform flow, Middleton (1966b) uses a modified Chézy equation:

$$U = C\sqrt{RS} \qquad (8)$$

where U is the velocity of uniform flow, C the modified Chezy coefficient (a rate of discharge coefficient), R the hydraulic radius and S the bottom slope. The Chézy coefficient is given by:

$$C = \frac{8g(\Delta\rho/\rho_f)}{f} \qquad (9)$$

where 'f' is the total friction coefficient which includes both the resistance to the flow from the bottom and sides of channel (fo) and from the fluid interface (fi). The total resistance coefficient 'f' is given by the following formula:

$$f = f_o + \left(\frac{w}{w+2d}\right) f_i \qquad (10)$$

where 'w' is the width of the channel and 'd' is the depth of the uniform underflow. The value of fo may be predicted from a Moody diagram such as found in fluid mechanics textbooks (ex. V. Streeter, 1966; Fluid Mechanics, McGraw-Hill). The value of fi may be predicted semi-quantitatively: fi should be proportional to $Re^{-\frac{3}{5}}$ (Lofquist, in Middleton 1966b). In the experimental part of this thesis fi is taken inversally proportional to the square root of the Reynolds Number ($fi = 1/\sqrt{Re}$).

3. Particle Movement

In general, no single shape factor is sufficient to explain the movement of a particle. Briggs and Middleton (1965) note one fundamental difference between the behaviour of particles moved by suspension and by rolling: "In suspension, the more spherical particles settle at the same rate as larger less spherical particles. In traction, the more spherical particles are moved along with smaller less spherical particles." The

above distinction can be used as a guide in discriminating between sediments deposited from suspension and those deposited after movement by traction.

An estimate of the competency of turbidity current flow (that is, its ability to transport coarse material) is given by the critical threshold stress (Komar, 1970).

$$\tau_{t_o} = 0.06 (\rho_s - \rho_t) g D \qquad (11)$$

where τ_{t_o} is the critical threshold stress at which the current will rotate the particle at rest to be transported, D is the diameter of the grains greater than about 7mm, ($\rho_s - \rho_t$) is the density difference between the grains and the turbidity current and 'g' is the gravitational constant. The equation can be used as long as the bottom sediment grains are larger than the sediment grains in suspension by one order of magnitude and providing the density of the turbidity current is low.

To approximate the flow velocity needed to yield the threshold stress, Komar (1970) uses

$$\bar{u} = \left[\frac{\tau_{t_o}}{C_f \cdot \rho_t}\right]^{\frac{1}{2}} \qquad (12)$$

where C_f is the drag coefficient taken as 0.0035 in his calculations. Applying equations (1) and (2), the required stresses and velocities found are shown in table 2.

Table 2

Minimum stresses and velocities yielded by turbulent flows (after Komar, 1970).

D cm	ρ_t g/cm^3	$\bar{u}$ cm/sec	τ_{to} dyne/cm^2
2	1.10	220	180
2	1.18	200	170
20	1.10	690	1.8×10^3
20	1.18	650	1.7×10^3

Gravels 2 cm in diameter are common in the base of graded beds, whereas in the Coheny channel, California, clasts of 20 cm in diameter are ordinarily found.

The above data indicate that low-density turbidity currents have the competency to transport the cobbles found in turbidites without appealing to semi-catastrophic events or very high density flows.

4. The Head of the Turbidity Current

The head which is the frontal, wedge-shaped part of the turbidity current flow was well described from flume experiments by Middleton (1966a). He found that the velocity of the head remained almost constant until nearly all the sediment had been deposited, when there was a sharp decrease in velocity. This gave rise also to a parallel sharp decrease in the thickness of the bed.

Within the head the flow rises and radiates. The head is followed by a wave in some experiments with low-density suspensions. The wave supplies the head with particles and little deposition occurs between the head and the ensuing wave.

The head itself is an agent of erosion. Flutes according to Middleton (1966a) are likely cut by the sediments moving within the head; deposition of sediments occur behind the head.

The following two equations were proposed by Middleton (1965) to account for the initial velocity of the head in his experiments:

$$V_o = 0.44\sqrt{\Delta\rho g H} \qquad (13)$$

where V_o: initial velocity of the head;

H: depth of water;

$\Delta\rho$: density difference between the suspension and the water;

g: acceleration due to gravity.

The velocity of the head, V, was also related to the maximum thickness of the head, d2:

$$V = 0.75\sqrt{\Delta\rho g d_2} \qquad (14)$$

Middleton (1965, p. 9) proposes the following equation to determine the velocity ahead of the flow (just above the bottom zone of strong boundary effect):

$$\log_{10}\frac{u}{V} = -0.93\frac{x}{d_2} \qquad (15)$$

where 'u' is the velocity in front of the flow, 'V' is the velocity of the head, 'x' is the distance from the head, and 'd_2' is the maximum thickness of the head. At a distance of one head height in front of the head, the velocity of the water near the bottom is roughly $\frac{1}{10}$ the velocity of the head and $\frac{1}{100}$ the velocity of the head at two head heights away.

A rapid way to determine roughly the velocity of the head of a turbidity current is to use a nomograph (Middleton, 1966a). Results are similar to those obtained in table 2 (page 18) from Komar's data on the velocities of natural turbidites.

5. Mechanism of Deposition

When a turbidity current travels down a channel the internal and boundary drag effect decreases the momentum of the current. When the ratio of u/w (where u is the average fluid velocity and w the fall velocity) is less than 40 or even 20, suspension is not fully developed and sediment begins to be deposited (Bagnold, 1962).

In flume experiments the initial suspension in the mixing box, which furnishes hydrostatic pressure to drive the current, diminishes in height thereby decreasing the velocity and causing deposition.

After working for several years with flows at low and high concentrations of salt and with plastic beads, Middleton (1967) recognized four main stages of accumulation for each resulting type of turbidite, only the last stage being the same for both kinds of flows.

In low concentration flows the stages are (i) deposition of a small amount of sediment just behind the head, followed by very little traction; (ii) slow accumulation of sediment with increasing traction; (iii) rapid deposition of the sediment with falling velocity after the main 'wave' of the current head has passed; and (iv) very slow deposition of the finest particles from the 'tail' of the current.

In the high concentration flows the bed accumulates by: (i) rapid deposition of most of the sediment with the top of the bed not clearly defined; (ii) waves at the upper surface of the fluidized upper two-thirds of the bed produce a continuous shearing motion and a circular churning motion within the bed; (iii) as the waves disappeared the bed consolidated with a smooth upper surface; and (iv) very slow deposition of the finest particles from the 'tail' of the current.

The velocity of the head remained roughly constant for both types of flows during deposition. When the bulk of the sediment was deposited, there was a sharp decrease in the velocity and thickness of the bed.

6. A Model Turbidity Current

Komar (1969) depicts a mathematical model of a turbidity current starting with an initial velocity of 407 cm/sec, a thickness of 32 m and a density of 1.12 g/cm^3. The parameters used in modeling the turbidity current flow are shown in table 3 and were derived from the South Pond data in the Mid-Atlantic Ridge.

Table 3

Parameters of a model turbidity current flow (after van Andel and Komar, 1969).

Ratio of size of walls to basin floor	0.10
Distance across basin floor	10,000 m
Density of current at start	1.12 g/cm^3
Density of current in second passage	1.09 g/cm^3
Thickness of flow at start	32 m
Fine mode, 70%	7.5 phi
Coarse mode, 30%	3.25 phi

The changes in average velocity, thickness of the coarse mode distribution and average density are shown in figure 3.

C. THE TURBIDITE

1. Bed Thickness

The sedimentation unit is the turbidite bed: it contains a single self-contained episode or event, i.e., the turbidity flow (Pettijohn, 1957).

In laboratory flume experiments the thickness of the bed is in the order of centimeters, whereas, in nature, the bed thickness is in the order of decimeters and meters. Middleton (1967) reports that the thickness of the bed remained almost constant close to the gate where the head of the flow had an almost steady velocity.

Increase in the volume of the suspension in the box, at constant concentration, increased the distance of travel of the flow. Middleton (1967) explains that,

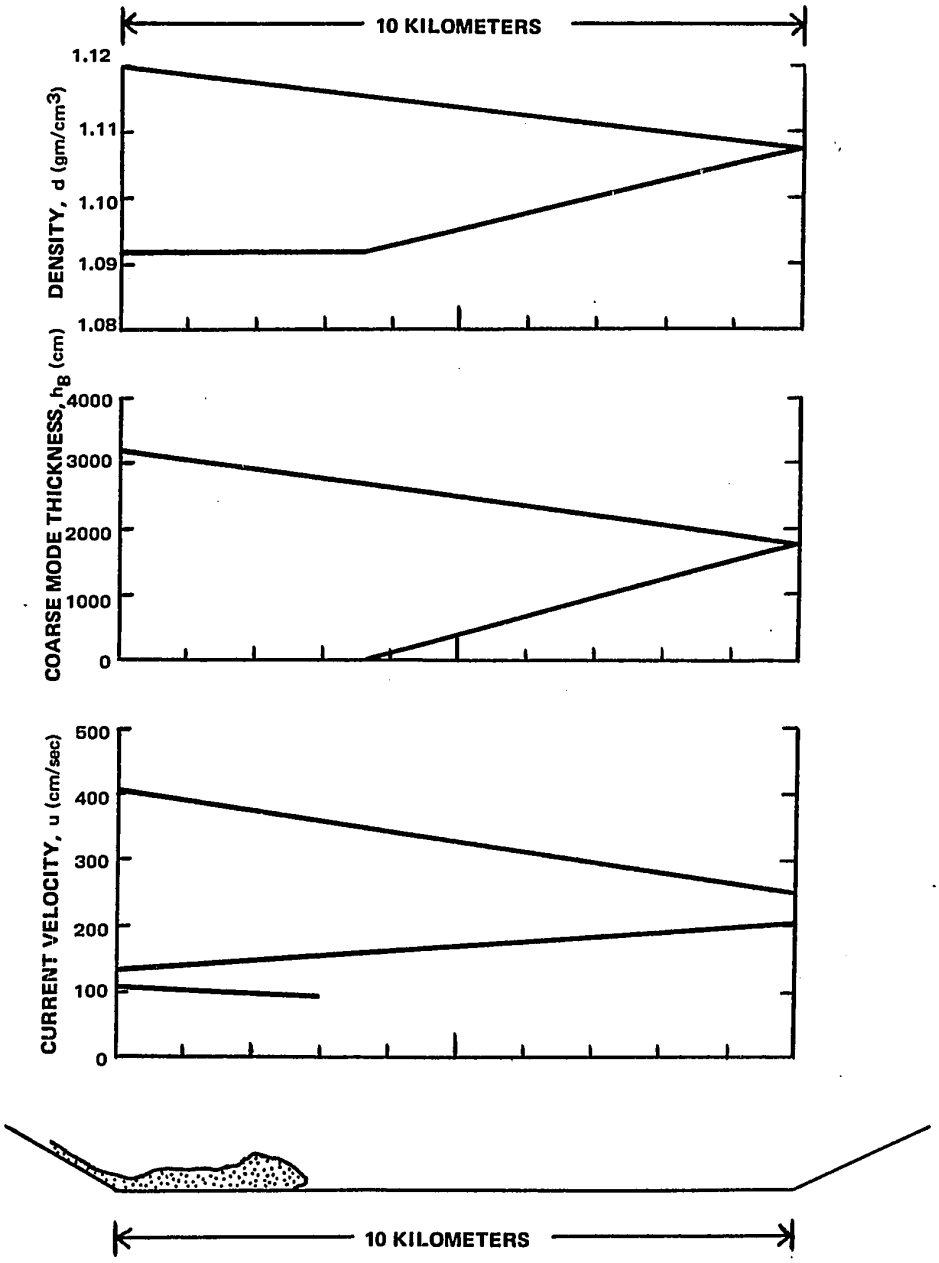

Figure 3. Progressive changes in average velocity, thickness of the coarse-mode distribution within the flow, and average density of a model turbidity current starting with an initial velocity of 407 cm/sec, thickness of 32 m, and density of 1.120 gm/cm^3 (from figure 14 in van Andel and Komar, 1969).

> "the increased volume of suspension is mainly used to enlarge the volume of the 'wave', which travels behind the head and supplies the head with suspension, thus permitting a proportionately greater distance of travel for the head and a proportionately greater length of bed deposited. The volume of suspension left behind the 'wave', per unit length of flume, apparently does not vary much with H (the height of the suspension in the mixing box). It is not entirely clear, however, why this should be true".

Increase in the initial concentration, at constant volume, increased both the thickness and the length of the bed.

2. Grading, Sorting and Skewness

Sediments in a turbidite formed by the sudden release of a suspension into a horizontal flume display both vertical and lateral grading. However, there is a difference in the type of grading formed by a bed deposited by a low concentration flow from one deposited by a high concentration flow (Middleton, 1965). The low concentration flows deposited turbidites displaying 'normal' grading, from coarse at the bottom to fine at the top. The beds deposited by high concentration flows were characterized by 'coarse tail' grading, in which a strong size grading was shown only at the top of the beds. The only consistent grading from coarse at the bottom to finer at the top was displayed by the very coarsest part of the distribution. A non-graded deposit forms when a current is fed for some time at a constant rate (Kuenen and Menard, 1952).

The sediment in proximal deposits are less well sorted than in the distal deposits. Sorting generally improves upwards, even when the median size does not decline going up. Sorting also improves away from the gate for both types of flows. The sorting of sediments with respect to size, shape and density can partially explain structures. The fall velocity of

the particles, turbulent diffusion, gravitational sliding and the shear stress of the channel are factors which affect sorting (Brush, 1965).

Grains within the samples just above the base often display positive skewness and attain their maximum skewness at the center of the bed. Still upwards, the skewness decreases to become usually negative at the top (Middleton, 1966a).

There is a decrease in grain size away from the lock in low concentration flows; whereas, in high concentration flows, only the basal portion of the turbidite shows a slight lateral grading.

Grain orientation, in the turbidite, parallel to the flow was observed by Middleton (1967) by using blue tracer particles which rested on the bottom of the channel.

3. Structure

Many structures found in turbidites can be explained by the competence of the flow, especially the head, which exerts sufficient stress to cause grooving, fluting and the disruption of the bottom beds as represented by the presence of large shale intraclasts in the turbidite (Komar, 1970). The flutes are probably cut by the erosive head: sediment deposition occurs some distance behind the head and not in the head itself (Middleton, 1966a).

The existence of tool and flute marks may be explained by the mechanism of inflow of the ambient fluid into the region of the head of a turbidity current through clefts and tunnels spaced out along the overhanging face (Allen, 1971). The flow velocity of the ambient fluid into the tunnels is

substantially smaller than that of the current into the fingers that lie between the tunnels. The ensuing spatial periodic variation of bed shear stress provides an explanation for the flute marks on the sole of turbidites according to the same author. The system of oppositely rotating longitudinal vortices for the three-dimensional flow into the head may explain the criss-crossing of tool marks found in turbidites (Allen, 1971).

The transporting competency of a turbidity current was well depicted by Kuenen and Migliorini (1950): a current with a density of 2, rolled along the bottom fragments several thousand times the weight of the largest grains shifted by a current of clear water with the same velocity. For a current density of 1.5, the factor drops to a few hundreds.

The sudden deposition of overburden on a mobile base may produce convolute laminations and irregular pockets of the upper bed in the underlying bed. Kuenen and Menard (1952) report that, "Contemporaneous deformations in graded graywackes and deep sea sands may be due to slumping, drag exerted by the following current, or sudden placement of overburden on very mobile deposits."

An array of structures found in natural turbidites have been duplicated by laboratory experiments using plaster of Paris and charcoal dust (Dzulinski and Walton, 1965). Wave-like undulations are better shown by fine-grained debris. Dune-like bed forms and deformations by impacting blocks are found associated with maar volcanoes (Fisher and Waters, 1970).

Diagenetic load casts of Pb-Cu-Ni-Co- minerals in lumps have been found in graywackes (Amstutz and Bubenicek, 1967). Current bedding around load casts, nodules in shaly siltstone as well as laminations with sphalerite and quartz are all structures which could be partly attributed to former turbidity currents (Schneider, 1964 and Schulz, 1964).

D. MODELING TURBIDITY CURRENTS

Model laws for the scaling-down of density and turbidity currents have been treated by Middleton (1966c). The two principal rules for scaling-down turbidity currents are that the Froude number and the ratio w/u

$\frac{\text{settling velocity}}{\text{average velocity}}$ be identical in the model and in the prototype.

1. Froudian Similarity

Froudian similarity of the model and the prototype is important to ensure similarity of flow regime.

The resistance to the flow of the turbidity current comes mainly from the bottom and sides of the channels, f_o , and is generally greater in the experimental flume than in nature. A greater resistance to flow decreases the velocity. To preserve Froudian similarity the slope in the model should be slightly greater than in the prototype.

When the Froude number is greater than unity, the flow is rapid and there is considerable mixing of the flow with the ambient fluid and a steady, uniform flow is not possible because the density of the flow decreases and the thickness increases in the down-flow direction (Middleton, 1966c).

Table 4

Froude numbers of turbidity currents

Locality and information	velocity u, cm/s		g cm/s^2	depth d, cm	Froude number
Lake Mead, U.S.A.					
Middleton, 1966b	15	.05/1.05	980	153	0.18
Menard, 1964	25	.06/1.06	980	100	0.34
Grand Banks, Nfld					
Menard, 1964					
1) sheet flow					
cables H-I	2310	.6/1.6	980	2000	2.70
	2310	.1/1.1	980	6400	3.06
cables I-J	820	.6/1.6	980	1200	1.23
	820	.1/1.1	980	4900	1.24
cables J-K	720	.6/1.6	980	1000	1.19
	720	.1/1.1	980	4100	1.19
2) flow in channels					
cables H-I	2000	.1/1.1	980	4600	3.12
I-K	930	.1/1.1	980	3000	1.80
Cascadia channel					
Pacific, 127°W,45°N					
Hurley, 1964					
channel mile,					
120	448	.05/1.075	980	6405	0.83
238	991	"	980	25620	0.91
361	717	"	980	21655	0.72
395	351	"	980	14640	0.43
460	823	"	980	16470	0.94
1280	296	"	980	5490	0.59
Mathematical model					
North Pond, 22°N					
Atlantic					
van Andel and Komar					
1969	1000	.175/1.20	980	1000	2.64

For unsteady flows, Keulegan (in Middleton, 1966c) introduces the dimensionless term ut/d, where ' u ' is the velocity, ' t ' is time and ' d ' is thickness of the current, to take into account the decrease in time scale in the model. Middleton (1966c, p. 204) states that, "If the model is to be 1/100 scale, and if the density difference is to be the same in the model as in the prototype, Froude similarity requires that the velocity in the model be reduced to 1/10 of the velocity in the prototype, and consequently the time scale in the model must also be reduced to 1/10 of the time scale in the prototype".

Froude numbers have been calculated for a number of natural turbidity currents in table 4.

2. The ratio of settling velocity to average velocity, ω/u

To take into account the behaviour of sediment in suspension within a turbidity current it is necessary to consider other variables: the mean diameter, the sorting coefficient, the volume concentration and the viscosity of the fluid. Usually a simplification is made in that the hydrodynamic behaviour of particles can be accounted for by their settling velocities ω measured at the average concentration in the turbidity current.

The settling velocity should be scaled down proportional to the average velocity. If the average velocity is 1/10 of the real velocity then a grain size which has a settling velocity 1/10 of the natural should be used (Middleton, 1966c).

By increasing the proportion of clay-sized particles at the expense of sand, the largest grains may behave as though they were suspended in a fluid whose density and viscosity is effectively that of the suspension of smaller grains (Kuenen, 1950). Commenting on the load transported by rivers, Bagnold says that, "While the discharge or transport rate of the coarser grades (of particles) is found to be a function of stream flow, that of the finer grades appears to be unlimited". The critical grain size below which these anomalies occur is usually put at 50 microns for sediments of natural mineral density (Bagnold, 1962). As a consequence, higher density turbidity currents can be formed because the effective settling velocity of the particles is considerably reduced by the presence of fine clays, and a correct scaling down of the factor ω/u is achieved without greatly reducing the size of the sediment from that of the prototype. Turbidity currents with a density as high as 1.91 were obtained in the large flume, in this thesis, because 24 % of the particles were composed of ilmenite having a grain diameter smaller than 44 .

If a low density turbidity current is modeled, the use of a high concentration slurry will produce a distorted model because of the non-Newtonian behaviour of the suspension, reduction of the turbulence, psuedo-plastic and dilatant behaviour of the water sediment mixture, thixotropic behaviour and many other poorly understood phenomena (Middleton, 1966c). This is why Middleton (1965, 1967) scales down the density of his sediment (plastic beads) to achieve the similarity in the ratio ω/u between the model and the prototype.

3. Limitations of small-scale experiments

Complete similarity between two flows is achieved if there is geometric similitude between the two flows and kinematic similarity at similar points in the flows. Years of work in dimensional analysis and in the modeling of open channel flows have shown that it is impossible to model all aspects of a fluid-sediment system simultaneously (Middleton, 1967).

In general, complete similarity is impossible and all the forces cannot be proportional in flow 1 and 2. In each case of similarity certain factors are less important than others and may be neglected. Only the most important variables should be taken into account in the model and in the prototype. Restricted similarity is then achieved. For example, to study the flow paths of turbidity currents in a model basin, it is best to use suspensions of clay or even salt solutions. If depositional processes are the object of study, sand or silt-sized particles are needed. The two main quantities to be kept under control are the Froude Number and w/u, which takes partly into account the behaviour of sediment in suspension.

The flumes utilized in the investigation of heavy mineral behaviour in experimentally produced turbidite beds do not have geometric similarity with the submarine topography where natural turbidity currents flow. The model is then said to be distorted in a fluid-mechanics sense. Distorted models are used in the studying of phenomena such as turbulence, cavitation, roughness of walls and turbo-machines configuration.

The results of this study should therefore not be viewed as representing accurately what happens to heavy minerals in natural turbidity currents, but rather should be considered a qualitative representation of what happens in nature.

Plate 1. Flumes utilized; the corer is at the end of the small flume.

CHAPTER IV

The Experiments

A. MATERIALS USED

1. Flumes

Two flumes were used: the larger measured 234.5 cm long x 30.5 cm high x 14.6 cm wide (78 5/8 in. x 12 in. x 5 3/4 in.). It was built of one-half inch thick waterproof plywood. It had a vertical sliding partition at 34.5 cm (13 1/2 in.) at the upper end and a water outlet at the lower end. The smaller flume was 156 cm long x 25 cm high x 7.1 cm wide and had a vertical partition at 41 cm. It was built of plywood except for one wall which was made of 1/4 in. thick plexiglass as shown in plate 1. The down-flume end was extended by a J-shaped galvanized tin pipe which served as a shock absorber for the incoming turbidity current, thus allowing minor reshuffling of the deposited sediments only at the farthest end of the flume. The interior wall of the flume was painted orange and subdivided by perpendicular lines at 5 cm intervals.

The optimum dimensions of the smaller flume were determined empirically by moving boards parallel to the edges of the larger flume to vary the width of the flow and by doing preliminary experiments with plaster of Paris, sphalerite, ilmenite and water.

2. Physical properties of the sediment

The following U.S. Standard sieves were used:

mesh no.	opening, micron
70	210
100	149
140	105
200	74
325	44

In addition a 200 BSS sieve (76 micron opening) was used for the ilmenite slag. Quartz sand of 100 mesh, means quartz particles that are retained by the 100 mesh sieve after passing through the preceding sieve number, 70. Alternately, it may be written: quartz sand of mesh -70, + 100 to indicate the above grain size.

The determination of particle size range of ground ilmenite with a diameter smaller than 44 micron was made with an hydrometer at Tioxide of Canada, Sorel. 5, 10 and 20 microns particles are estimated by settling for specified times and depths according to the Stokes formula:

$$\omega = 2/9 \left(\rho_1 - \rho_2 \right) \times d_2/4 \times 980/\eta \quad \text{cm/sec}, \qquad (16)$$

where,

w= settling velocity of spherical particles, cm/sec

ρ_1 = density of ilmenite, 4.7 g/cm 3

ρ_2 = density of water or suspension medium, g/cm 3

d= diameter of particle, cm

η = viscosity of water or suspension medium.

Settling times used are:

5 minutes for 20 microns particles
15 minutes for 10 microns particles
60 minutes for 5 microns particles

The settling velocities of the quartz particles were derived from Rubey's diagram (see a handbook of applied hydrology such as Ven Je Chow, 1964, Handbook of applied hydrology, McGraw-Hill) and they checked well with the velocities obtained by sedimentation through a vertical column.

The size fractions and the settling velocities of quartz and ilmenite is given in table 5.

TABLE 5

Size and settling velocity of sediment

Ilmenite slag			Quartz		
weight, P%	size microns	settling vel. w, cm/sec	weight P%	size microns	settling vel. w, cm/sec
3.2	76	1.16	18.0	210	2.3
5.1	44	0.39	46.4	149	1.3
42.5	20	0.08	35.1	105	0.8
21.8	10	0.02	0.5	74	0.4
13.7	5	0.005			
13.7	-5	0.0008			

Once the size fractions are shown, properties, such as specific gravity, diameter and fall velocity can be determined for each size fraction. As a turbidite comprises many different particle sizes, and, in most cases, more than one mineral, weighed values are obtained for the diameter, fall velocity and specific gravity.

The weighed diameter, $\overline{d}$, is given by:

$$\overline{d} = \frac{P_1\% \; d_1 + P_2\% \; d_2 + \ldots P_n \% \; d_n}{100} \qquad (17)$$

and gives a value of 150 microns.

A quartz to ilmenite ratio 5:1, by volume, was used in the experiments in the large flume. Quartz has a density of 2.64 and ilmenite, a density of 4.7 as determined by using a pycnometer. The weighed density, $\bar{\rho}$, of the particles is given by:

$$\bar{\rho} = (\%\ \text{ilm, wt} \times \rho\ \text{ilm}) + (\%\ \text{qtz, wt} \times \rho\ \text{quartz}) \qquad (18)$$

A value of $\bar{\rho}$ of 3.18 is obtained.

In a similar fashion, the weighed settling velocity $\bar{w}$, for all the particles is given by:

$$\bar{w} = \frac{P\ \%\ w_1 + P_2\ \%\ w_2 \ \ldots\ Pn\%}{100} \qquad (19)$$

and results in a weighed mean fall velocity of 1.1 cm/sec.

Quartz sand (Shell no. 90 of the 3M Company) was used in the experiments. Canadian Titanium (Varennes, Quebec) supplied the ilmenite slag. The ilmenite sand was obtained from Tioxide of Canada (Sorel, Quebec).

B. EXPERIMENTAL PROCEDURES

1. Determination of Density

Determination of the initial density of the mixture in the lock was obtained by weighing the sediments in a large cylinder and adding a known amount of water. The mixture was then poured to the five-liter mark (18 cm high) in the lock. In the large flume, a known amount of water and sediments were poured into the lock, and then water was added to the ten-liter mark (20 cm high). The density of the resulting slurry was calculated.

2. Watertightness

To prevent movement of fluid from one side of the vertical sliding partition to the other, rubber stripes were sandwiched on both sides of the plexiglass panel. Water and sediment-water mixtures were poured so as to maintain about equal pressure on either side of the partition.

3. Release of the Mixture

When the water was calm in the flume, sediments and water were thoroughly mixed by random motion of the hand. The vertical panel was then quickly pulled upwards and a chronometer timed the flow. When the head of the turbidity current reached the end of the flume, the chronometer was stopped.

4. Draining the Water

The turbidite was deposited within half a minute from the time the partition was released. A waiting period of one hour or more was allowed for the settling of the bulk of the smallest suspended particles. The water was then drained by opening a valve at the lower end of the flume and by siphoning it out with a small hose. Part of the suspension-deposited ilmenite was drained away with the water; but the sediments deposited from the turbidity current all remained in place.

A waiting period of one day to one week was needed depending on the thickness of the bed, for the turbidite to evaporate sufficient water to reach a consistency where it could be sampled.

5. Sampling the Turbidite

The turbidite was sampled with the piston corer shown in plate 1. The piston was a brass rod threaded into a disk of teflon; the cylinder, 25 1/2 cm long by 2.2 cm inside diameter, was made of glass or transparent plexiglass tubing.

Samples were taken in the larger flume at the 10, 50 and 90 cm-positions. Two samples were taken at each site and were arbitrarily subdivided into a number of equal width, horizontal slices according to the thickness of the sample. This technique was used by Emery and his associates in sampling the middle of San Pedro basin (Menard, 1964 p. 216).

The upper portion of the thinnest samples was removed with a spatula because it contained the suspension-deposited ilmenite layer. The lower part of the thin cores was deposited while the turbidity current was flowing and is thus considered in the analysis of the results.

The thickness of each bed was recorded at sampling time when sufficient water had evaporated to permit each core being taken out without flowing (too much water) or crumbling (too dry). The beds, of course, had slightly reduced in thickness since the time of deposition, but all the beds had a similar consistency in order to be sampled.

The top of the turbidite generally formed a plane surface through all the length of the flume.

6. Analysis of the samples

Samples destined for grain-size analysis were first completely dried.

When an electronic particle-counter was used, sample drying was not required.[1] The electronic counter, although very accurate and extremely fast and reliable for most small sized particles - about 1 to 500 microns in diameter found in natural sediments, was not used because ilmenite does not mix homogeneously with quartz sand even when using a small glass stirrer and a glycerine-saline solution to keep the sediments in suspension.

Each sample was pressed into a disk in order to compute the percentage of quartz and ilmenite by x-ray fluorescence.

C. EXPERIMENTAL RESULTS

Introduction

A series of experiments (nos. 1 to 10, table 7) was made at different densities in the large flume using a fixed ratio of quartz to ilmenite slag. Velocities of the turbidity currents were measured and standard deviations were calculated. An equation showing the relationship of velocity with the density of the initial slurry was derived. Samples of the sediments were analysed by X-ray fluorescence to determine the ilmenite content.

Following this, a series of six runs was made in the small flume. In the first three runs (S-1, S-2, and S-3) a higher proportion of

---

1. Coulter counter, supplied by Coulter Electronics, Florida, Montreal.

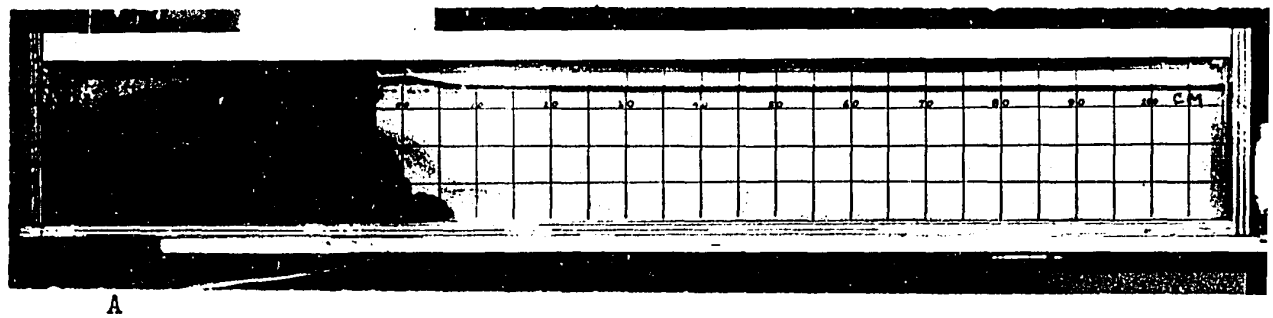

A

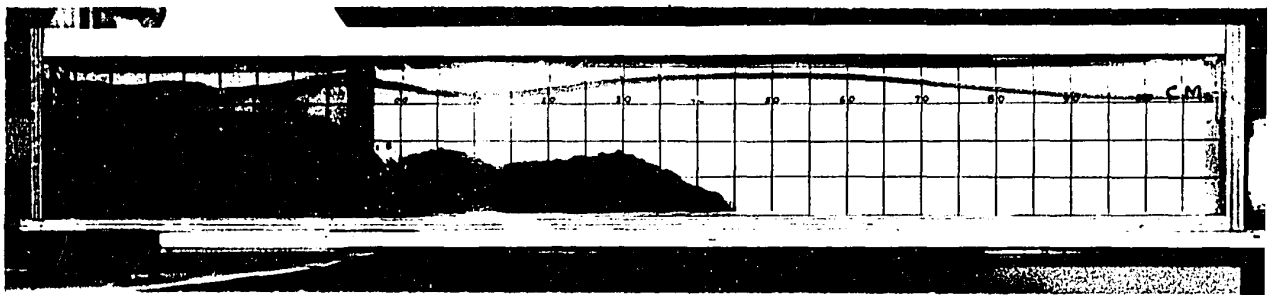

B

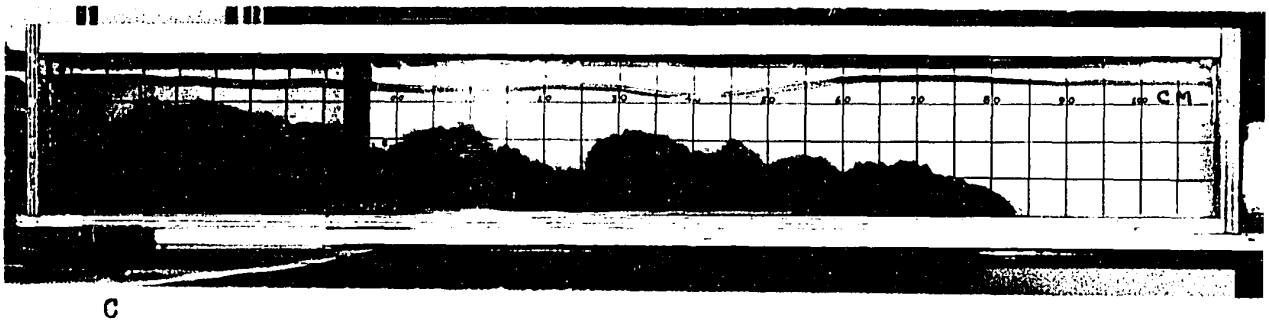

C

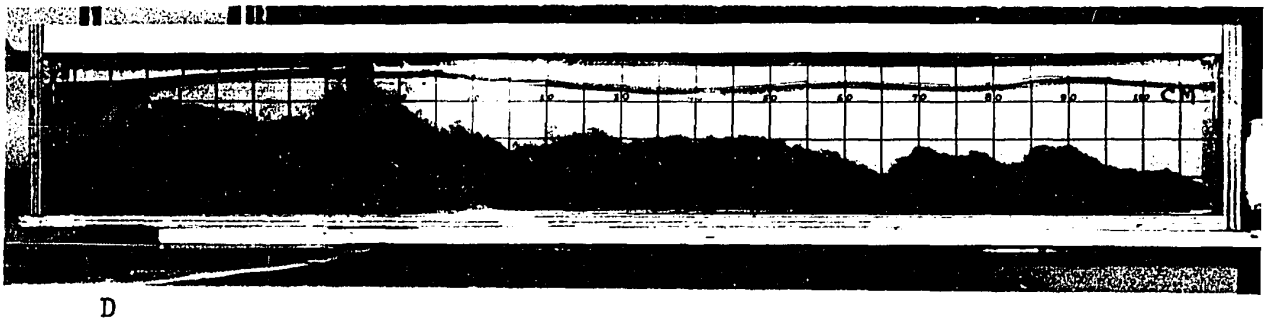

D

Plate 2. Turbidity current

A: release of the slurry; ratio of quartz to ilmenite 85:15, d= 1.24.

B: advance of turbidity current and formation of a wave on water surface.

B, C, D: illustrate the formation of eddies behind the head.

D: turbidity current as it reached end of flume; time of flow from A to D: 5 seconds.

fine-grained materials was used. In the last three runs (70, 100, and 140) a fixed ratio of quartz to ilmenite with the same grain size was used in each run.

Finally, experiments (A and B) in which quartz and ilmenite had the same average fall velocity were performed in the large flume using two different quartz to ilmenite ratios. Thick cross-sections of the sediment were collected for microscopic study.

Additional experiments were run to take photographs of a turbidity current.

The small flume was constructed after the experiments with the large flume had been completed.

The small flume had the advantage of yielding thick turbidites while using a small amount of initial suspension which in turn can be analysed more easily. Operation was also simpler, the initial slurry homogenized faster. But the similarity of flow conditions with natural turbidity currents is exaggerated especially with respect to fo, the resistance from bottom and sides of the channel to the flow. The ensuing decrease in the velocity of the flows causes both the Reynold's and the Froude numbers to be smaller. The Reynold's number is also decreased due to the smaller hydraulic radius, R.

The plexiglass front of the smaller flume permitted better observation of the advance of the turbidity current and in the taking of photographs.

The density, mean velocity and temperature for each flow are shown

Table 6

Physical Parameters For The Flows

Experiment number (1)	Density g/cm^3	Temperature °C (2)	Velocity cm/sec	average	2	(3)
1	1.065	12.0	9.0	9.0		
2	1.130	21.9	15.5	15.5		
3	1.195	14.6	22.2			
		8.0; 10.0	21.7			
		8.0; 6.0	22.7	22.0	0.9	
		8.0; 10.0	21.7			
		8.0; 10.0	21.7			
4	1.260	9.5	28.2	28.2		
4b	1.325	22.0	30.3			
		22.0	31.2	31.7		
5	1.390	22.0	35.9			
		22.0	35.9	35.9		
6	1.520	11.1	45.5			
		22.0	43.5			
		22.0	41.7	43.2	3.2	
		18.5	41.7			
		18.5	43.5			
7	1.650	12.0; 10.5	43.5			
		22.0	45.5	44.2		
		22.0	43.5			
8	1.780	11.6; 16.5	50.0			
		21.0; 23.0	50.0			
		19.0; 17.0	52.6	49.6	4.2	
		5.0; 17.0	47.6			
		5.0; 13.0	47.6			
9	1.910	10.8; 16.2	50.0	50.0		
10	2.040	12.5; 17.9	7.6	7.6		(4)

Table 6 continued

Experiment number (1)	Density g/cm³	Temperature °C (2)	Velocity cm/sec	average (3)	
S-1	2.00	25.5; 12.5	57.5	57.5	
S-2	2.45	24.4; 11.0	57.5	57.5	
S-3	1.43	18.0; 14.7	34.8	34.8	
70	1.24	18.1; 17.6	12.7	12.7	(4)
100	1.22	17.7; 17.2	10.6	10.6	(4)
140	1.24	18.6; 23.0	23.0	23.0	
A	1.195	7.0; 5.0 6.0; 5.0 5.0; 3.0	21.3 20.8 21.7	21.3	
B	1.195	9.0; 6.0 8.0; 4.0 7.0; 4.0	17.9 18.2 18.5	18.2	

Note (1) Experiments 1 to 10 incl. consisted of particles of quartz and ilmenite in the proportion 5:1 by volume respectively. Experiments S-1 and S-2 had equal volumes of ilmenite and quartz. Experiment S-3 had plaster of Paris, silica and sphalerite in the following proportions by volume, 2:2:1. Experiments 70, 100 and 140 had 85% silica compared to 15% ilmenite by volume. Experiments A and B had the fall velocity of ilmenite equal to the average fall velocity of the quartz sand. In experiment A the ratio of quartz to ilmenite was 5:1; whereas, in B the ratio was 9:1.

(2) Where two temperatures are shown, the first refers to the temperature of the initial mixture in the lock whereas, the second represents the temperature in the rest of the flume.

(3) is the sample standard deviation.

(4) Only a minor portion of the sediments in run nos. 10, 70 and 100 participated in the turbidity current.

Experiments S-1, S-2, S-3, 70, 100 and 140 were made in the small flume.

in table 6. Where two temperatures are shown, the first refers to the temperature of the initial mixture in the lock whereas, the second represents the temperature in the rest of the flume.

1. Experiments performed in the large flume

The first ten experiments were performed in the large flume. The volume ratio of ilmenite to silica was 1:5. Water in the flume stood at a height of 20 cm. Under these conditions, each kilogram of mixed sediments contributed to the density of the slurry by a factor of 0.065. The densities ranged from 1.065 to 2.040. The first nine experiments are considered, the last experiment being discarded because most of the initial slurry did not form a turbidity current.

The number of each sample of turbidite is given in table 7 along with the thickness of the bed at the sampling site. The amount of ilmenite is expressed in per cent and by a separation ratio (the relative amount of ilmenite found in one horizontal section compared to the amount found in the first slice resting at the bottom of the bed).

Table 7

Results from the runs performed in the large flume.

Run number	Sample number ②	Bed thickness, mm ③	Percent of ilmenite ①	Separation ratio
1	1, 1-2-X	2	17	0.59
(d= 1.065)	2 1-2-T		13	0.45
	3 1-2-B		29	1.00
	4 1-7-X	1	34	0.77
	5 1-7-T		27	0.61
	6 1-7-B		44*	1.00
	7 1-12-X	1-	54	
	8 1-17-X	1-	72	
2	9 2-2-X	5	29	0.69
(d= 1.130)	10 2-2-T		7	0.16
	11 2-2-M		10*	0.24
	12 2-2-B		42*	1.00
	13 2-7-X	2	36	0.67
	14 2-7-T		25	0.46
	15 2-7-B		54*	1.00
	16 2-12-X	1	49	0.82
	17 2-12-T		31	0.52
	18 2-12-B		60*	1.00
	19 2-17-X	1-	58	
3	20 3-2-X	8	27	0.67
(d=1.195)	21 3-2-4		13	0.32
	22 3-2-3		17*	0.42
	23 3-2-2		18*	0.45
	24 3-2-1		40*	1.00
	25 3-7-X	4	31	3.37
	26 3-7-T		(60)	6.52
	27 3-7-M		14*	1.52

Table 7 continued

Run number	Sample number ②		Bed thickness, mm ③	Percent of ilmenite ①	Separation ratio
3 (cont'd)	28	3-7-B		9*	1.00
	29	3-12-X	2.5	39	2.44
	30	3-12-T		(60)	3.75
	31	3-12-B		16*	1.00
	32	3-17-X	1	34.5	
4 (d=1.260)	33	4-2-X	8	29.5	1.84
	34	4-2-4		(55)	3.44
	35	4-2-3		25*	1.56
	36	4-2-2		18.5*	1.16
	37	4-2-1		16*	1.00
	38	4-7-X	6	30	1.87
	39	4-7-T		55	3.44
	40	4-7-M		23*	1.44
	41	4-7-B		16*	1.00
	42	4-12-X	4.5	37	1.95
	43	4-12-T		60	3.16
	44	4-12-M		22.5*	1.18
	45	4-12-B		19*	1.00
	46	4-17-X	2.5	37	1.32
	46A	4-17-T		51	1.82
	46B	4-17-B		28*	1.00
5 (d=1.390)	47	5-2-X	11	32	1.21
	48	5-2-4		52	1.96
	49	5-2-3		24*	0.91
	50	5-2-2		26*	0.98
	51	5-2-1		26.5*	1.00
	52	5-7-X	9	37	1.72
	53	5-7-4		(60)	2.79
	54	5-7-3		26*	1.21
	55	5-7-2		21.5*	1.00
	56	5-7-1		21.5*	1.00

Table 7 continued

Run number	Sample number ②	Bed thickness, mm ③	Percent of ilmenite ①	Separation ratio
5 (cont'd)	57, 5-12-X	8	33.5	1.52
	58 5-12-T		52	2.36
	59 5-12-M		16*	0.73
	60 5-12-B		22*	1.00
	61 5-17-X	8	27	0.96
	62 5-17-T		42	1.50
	63 5-17-M		27*	0.96
	64 5-17-B		28*	1.00
6 (d=1.520)	65 6-2-X	12	38	1.58
	66 6-2-4		63	2.62
	67 6-2-3		21*	0.87
	68 6-2-2		30*	1.25
	69 6-2-1		24*	1.00
	70 6-7-X	12+	30	1.67
	71 6-7-4		52	2.89
	72 6-7-3		25.5	1.42
	73 6-7-2		24	1.33
	74 6-7-1		18	1.00
	75 6-12-X	13	33	1.32
	76 6-12-4		44	1.76
	77 6-12-3		27*	1.08
	78 6-12-2		17*	0.68
	79 6-12-1		25*	1.00
	80 6-17-X	13+	24	1.37
	81 6-17-4		41	2.34
	82 6-17-3		25*	1.43
	83 6-17-2		23*	1.31
	84 6-17-1		17.5*	1.00
7 (d=1.650)	85 7-2-X	14	34	1.21
	86 7-2-4		48	1.71
	87 7-2-3		31*	1.11
	88 7-2-2		18.5*	0.66

Table 7 continued

Run number	Sample number ②	Bed thickness, mm ③	Percent of ilmenite ①	Separation ratio
7 (cont'd)	89, 7-2-1		28*	1.00
	90 7-7-X	17	33	1.20
	91 7-7-4		44	1.60
	92 7-7-3		28*	1.02
	93 7-7-2		23*	0.84
	94 7-7-1		27.5*	1.00
	95 7-12-X	19	32.5	1.10
	96 7-12-4		42	1.42
	97 7-12-3		24.5*	0.83
	98 7-12-2		30.5*	1.03
	99 7-12-1		29.5*	1.00
	100 7-17-X	20	26.5	0.98
	101 7-17-4		void	
	102 7-17-3		void	
	103 7-17-2		23*	0.85
	104 7-17-1		27*	1.00
8 (d=1.780)	105 8-2-X	22	32.5	1.12
	106 8-2-4		44	1.52
	107 8-2-3		30*	1.03
	108 8-2-2		25*	0.86
	109 8-2-1		29*	1.00
	110 8-7-X	22	36	1.20
	111 8-7-4		43	1.43
	112 8-7-3		34	1.13
	113 8-7-2		29	0.97
	114 8-7-1		30	1.00
	115 8-12-X	22	30	0.97
	116 8-12-4		45	1.45
	117 8-12-3		28.5*	0.92
	118 8-12-2		30*	0.97
	119 8-12-1		(31)	1.00
	120 8-17-X	20	void	

Table 7 continued

Run number	Sample number ②	Bed thickness, mm ③	Percent of ilmenite ①	Separation ratio
8 (cont'd)	121, 8-17-4		void	
	122 8-17-3		void	
	123 8-17-2		18*	0.58
	124 8-17-1		31*	1.00
9 (d=1.910)	125 9-2-X	23	30.5	1.17
	126 9-2-4		(40)	1.54
	127 9-2-3		22	0.85
	128 9-2-2		25.5	0.98
	129 9-2-1		26	1.00
	130 9-7-X	22	29.5	0.98
	131 9-7-4		40	1.33
	132 9-7-3		22*	0.73
	133 9-7-2		33*	1.10
	134 9-7-1		30*	1.00
	135 9-12-X	22-	33.5	1.22
	136 9-12-4		(40)	1.45
	137 9-12-3		23.5*	0.85
	138 9-12-2		34*	1.24
	139 9-12-1		27.5*	1.00
	140 9-17-X	20	32	0.98
	141 9-17-4		49	1.51
	142 9-17-3		32.5*	1.00
	143 9-17-2		(23)	0.71
	144 9-17-1		32.5*	1.00
10	Very little sediment participated in the turbidity current. Hence, no data was obtained from this run.			

Note (1) A number is enclosed within parantheses, under % of ilmenite, when the sample spattered on the hot plate. A sample that spattered violently is declared 'void'.
- The percent of ilmenite is given in weight %.

Table 7 continued

Note 2: (cont'd) In the descriptive sample number, the first numeral refers to the run number; the numeral between the two dashes refers to the sampling site given in decimeters below the vertical partition; the last numeral identifies the sample in the core starting by 'one' at the bottom. T: top, M: middle, B: bottom, X: average.

3: minus (-) means slightly less.

The richest samples of dense mineral deposited by the turbidity currents were found at the bottom of the bed in the first three low-density runs (see table 7). This is most clearly seen in run no. 2 which had a density of 1.130. The bottom of the core in this run, taken 12 decimeters below the vertical partition was the richest in ilmenite of all the runs, namely, 60% ilmenite. From run no. 4 (density = 1.260) onwards, the bottom samples followed no particular trend until runs 7 and 8, where the percentage of ilmenite tended to stabilize at about 29%.

Each bed was equally subdivided into horizontal slices as indicated previously. At the first sampling site below the gate, the second sample upwards from the bottom consistently increased in ilmenite content, from 10% to 30%. This phenomenon occurred in runs with densities up to 1.520 (run no. 6). The second sample upwards from the bottom steadily decreased in amount of ilmenite at the three first sampling sites in runs no. 5 and 6; this pattern was completely reversed for the last three denser runs, increasing in ilmenite content upwards.

The third sample up from the bottom showed very little consistency in ilmenite content in all the runs. However, in flows 6, 7 and 9 it displayed

a trend opposite to that of the second sample, the ilmenite content decreased upwards.

In experiment 7, at 7 decimeters downflume, a 2 mm-thick, horizontal, ilmenite-rich layer was present midway in the turbidite. This could be due to a change in the mode of deposition of the slurry. This enrichment phenomenon coincided with an increased thickness of the bed away from the gate, contrary to other runs (which were wedge-shaped away from the source) except run number 6.

Figure 4 shows a plot of the initial density of the flow versus the velocity of the head of the turbidity current. In order to find the margin of error of the velocities (data given in table 6), the sample standard deviation was calculated at experiment numbers 3, 6 and 8 where 5 runs were made at each experiment. Standard deviations were calculated using the formula:

$$\sigma = \sqrt{\frac{\sum_{i=1}^{n} (x_i - x)^2}{n-1}} \qquad (16)$$

where x_i is the velocity at run i, x is the average velocity, and n is the number of runs in each experiment. Using the values calculated from these 3 experiments, 95% confidence limit lines ($\pm 2\sigma$) were plotted for all the experiments. A more rigorous treatment of the data concerning the velocities is given in figure 5. A small error in timing the velocity of a run is amplified as the density of the initial slurry increases, because the velocity also increases.

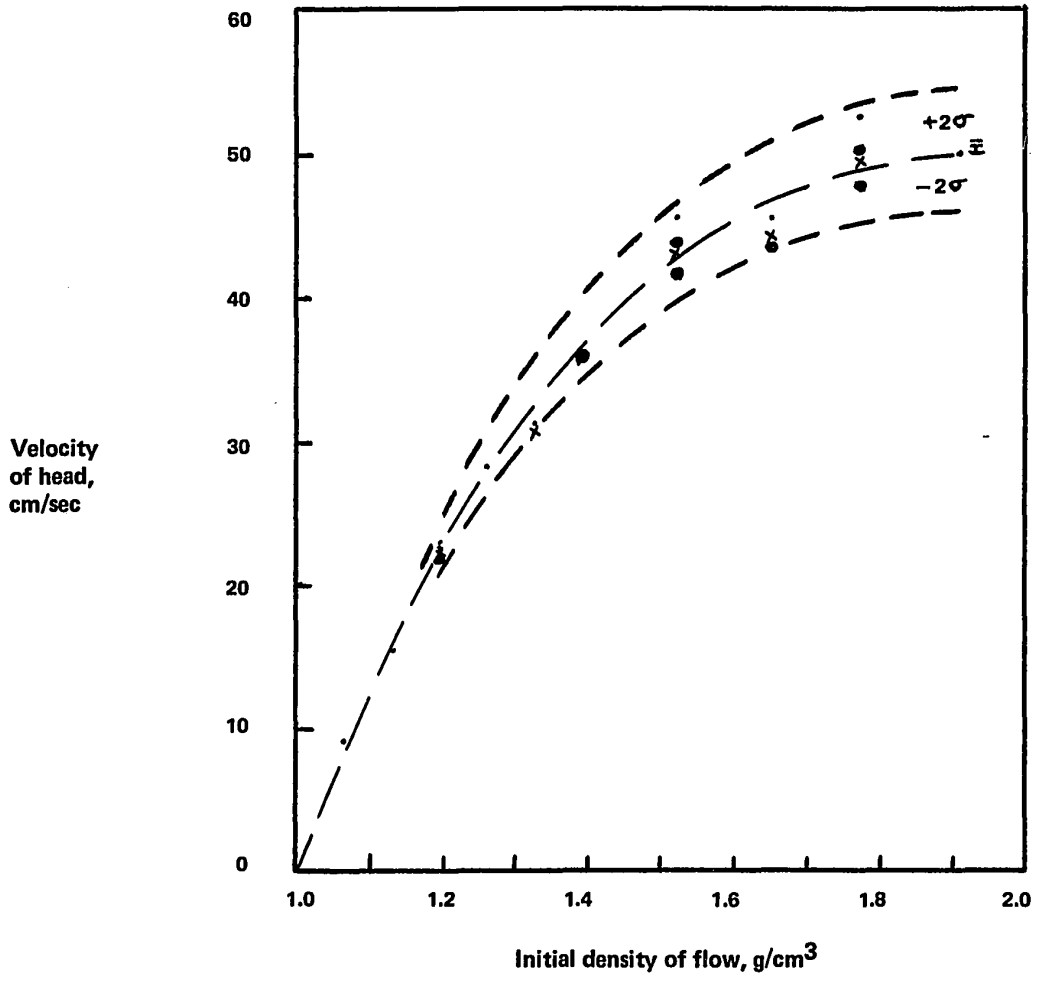

Figure 4. Sample standard deviation of the velocities. The data is taken from table 6. $\bar{x}$ is the mean velocity (center line) of the turbidity current and σ the sample standard deviation. A cross is the average value for all the runs in an experiment. Two velocities that coincide are represented by a solid circle and three velocities that coincide are indicated by a triangle.

A linear equation was computed to relate the velocity of the turbidity current to the density of the initial slurry:

$$\log_{10} u = -1.67 + 1.71 \log_{10} \sqrt{\Delta\rho / \rho_t \times g \times H} \qquad (17)$$

where, u is the average velocity of the turbidity current, $\Delta\rho$ is the difference in density between the initial slurry and water, ρ_t is the initial density of the flow, g is the gravitational constant and H is the height of the initial suspension, 20 centimeters in the large flume. The values for the estimated velocities are shown by the straight line in figure 5. The standard error of estimate is 2%. The term $\sqrt{\Delta\rho/\rho_t \times g \times H}$ is almost identical with the denominator of the Froude number, $\sqrt{\Delta\rho / \rho_t \times g \times d}$. The only difference being that H represents the height of the initial slurry and d, the thickness of the turbidity current. The term -1.67 might account partially for the resistance to the flow from the bottom and sides of the channel (f_o) and from the overlying fluid interface (f_i).

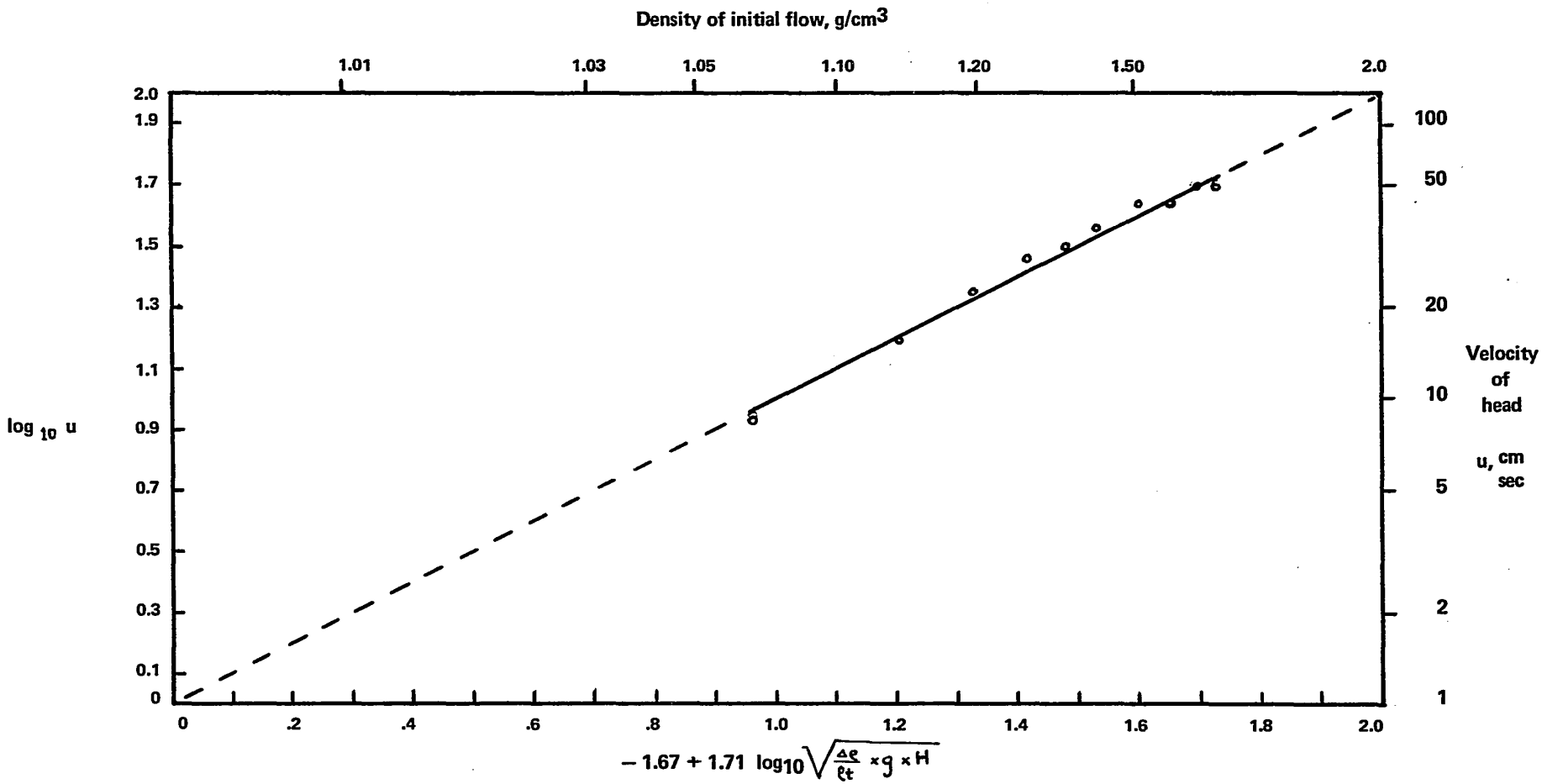

Figure 5. Estimated velocities for the runs performed in the large flume. u is mean velocity; $\Delta\rho$ is the difference between the density of the initial flow (ρ_t) and of water; g is the gravitational constant and H is the height of the initial suspension. Circles represent experimental values of velocity.

Table 8

Resistance to flow, Froude and Reynold's numbers.

Experiment number	Resistance Coefficients upper, f_i	channel, f_o	Total	Reynolds no. Re 10^{-3}	Froude no. Fr
1	.009	.035	.039	12.2	.37
2	.006	.032	.034	26.8	.46
3	.006	.032	.034	27.0	.55
4	.005	.031	.033	35.3	.63
4b	.004	.030	.032	53.2	.63
5	.004	.030	.032	62.2	.68
6	.004	.029	.031	68.5	.75
7	.004	.029	.031	70.7	.71
8	.004	.029	.031	70.0	.76
9	.004	.029	.031	65.1	.73
A	.006	.033	.035	24.3	.53
B	.007	.033	.036	22.3	.45
S-1	.005	.035	.037	46.4	.89
S-2	.005	.035	.037	45.6	.81
S-3	.006	.036	.039	30.0	.69
140	.006	.038	.041	24.2	.57

The depth of the underflow, d, is taken as 10 cm for the large flume and 8.6 cm for the small one. The hydraulic radius, R, is 4.2 cm for the large flume and 2.5 cm for the small one. Explanations on f_o, f_i, f, Re and Fr are given in section III.B.2. Experiments S-1, S-2, S-3 and 140 were made in the small flume.

Table 9 gives the calculated resistance coefficient, Froude and Reynold's numbers for each experiment performed in the large and small flumes. For experiment 1 through 9, the Reynold and Froude numbers generally increase with the initial density of the turbidity current.

It is also shown that the total resistance coefficient of the flow, f, (determined from equation 6) comes mainly from the channel bottom and sides, f_o, and very little from the upper fluid interface, f_i. This might be because the flows were tranquil (Fr 1). Figures 6 and 7 show the values for f plotted against Froude and Reynold's numbers respectively. The total resistance to the flow generally decreases with increasing Froude and Reynold's numbers, but stabilizes at a density of 1.520 (experiment 6) and higher.

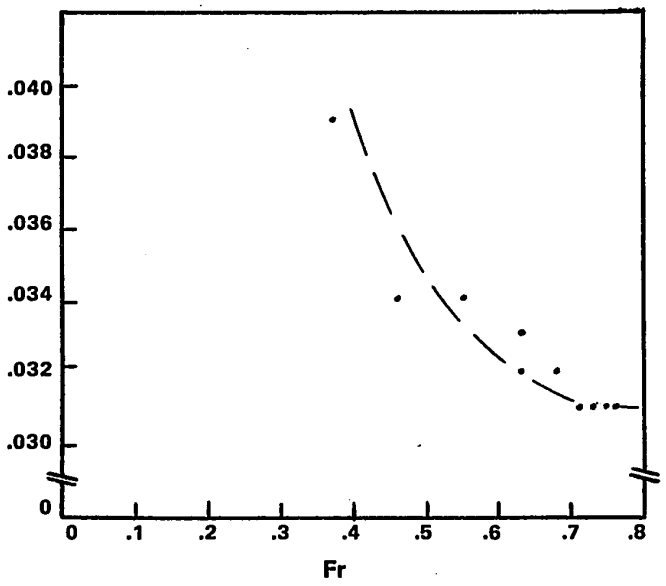

Figure 6. The total resistance coefficient plotted against Froude number for experiments 1 through 9.

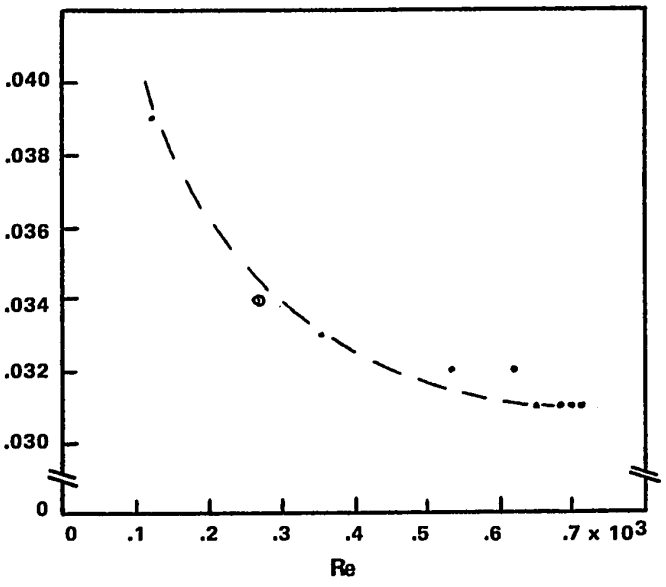

Figure 7. The total resistance coefficient plotted against Reynold's number for experiments 1 through 9.

2. Experiments in the small flume

Six experiments were made in the small flume (table 9). The first two runs, S-1 and S-2 contained equal volumes of ilmenite and silica. The third run, S-3, contained plaster of Paris, silica and sphalerite in the proportions 2:2:1 respectively.

In the last three experiments the numbers 70, 100 and 140 refer to the mesh size of the silica and ilmenite. These flows with a density of 1.24 were made to study the effect of grains size on turbidity flow. The grains consisted of 85% quartz and 15% ilmenite by volume.

The number of each sample of turbidite is given in table 9 along with the thickness of the bed at the sampling site.

Of the three first experiments in the small flume only S-1 produced a turbidite with a constant bed thickness. Runs S-2 and S-3, produced beds that tapered towards the lower end of the flume.

Broad waves of only a few millimetres in amplitude characterized the upper surface of the turbidite in run no. S-1. The wavelength was 7.5 cm near the lock and increased down-flume to slightly more than 10 cm. Flow no. S-3 which contained sphalerite, plaster of Paris and silica also displayed wavelets at the upper surface of the bed, but the wavelengths were much shorter, in the order of several millimetres up to a few centimeters. They also had a gentler slope on the lee-side. Clumps of coarser sediments with a size of 2 mm or more tended to form against the steeper side (up-current) of the wavelets.

Table 9

Results from the runs performed in the small flume.

Run number	Sample number ③	Bed thickness, mm ④	Percent of ilmenite ①	Separation ratio ②
S-1 (d=2.00)	145, S1-1-X	20	52	1.04
	146 S1-1-4		79	1.58
	147 S1-1-3		46	0.92
	148 S1-1-2		48	0.96
	149 S1-1-1		50	1.00
	150 S1-5-X	20	55	1.15
	151 S1-5-4		72	1.50
	152 S1-5-3		46	0.95
	153 S1-5-2		42	0.87
	154 S1-5-1		48	1.00
	155 S1-9-X	20	54	1.17
	156 S1-9-4		72	1.56
	157 S1-9-3		51	1.11
	158 S1-9-2		51	1.11
	159 S1-9-1		46	1.00
S-2 (d=2.45)	160, S2-1-T	48	50	0.86
	161 S2-1-5		52	0.89
	162 S2-1-4		55	0.95
	163 S2-1-3		55	0.95
	164 S2-1-2		58	1.00
	165 S2-1-1		58	1.00
	166 S2-5-5	35	57	1.08
	167 S2-5-4		59	1.11
	168 S2-5-3		57	1.08
	169 S2-5-2		57	1.08
	170 S2-5-1		53	1.00
	171 S2-9-T	22	63	1.07
	172 S2-9-M		63	1.07
	173 S2-9-B		59	1.00

Table 9 continued

Run number	Sample number ③	Bed Thickness, mm ④	Percent of ilmenite ①	Separation ratio ②
S-3 (d=1.43)	No samples taken: after four days the turbidite was still very soft.			
Mesh 70 (d=1.24)	174, 70-10-X	9	5.4	0.45
	175 70-10-4		void	void
	176 70-10-3		6.0	0.50
	177 70-10-2		3.1	0.26
	178 70-10-1		12.0	1.00
	179 70-50-X	2	0.7	0.87
	180 70-50-T		1.1	1.37
	181 70-50-B		0.8	1.00
	182 70-90-X	1-	1.2	
Mesh 100 (d=1.22)	183 100-10-X	11	6.5	0.60
	184 100-10-4		1.2	0.11
	185 100-10-3		4.8	0.44
	186 100-10-2		8.7	0.81
	187 100-10-1		10.8	1.00
	188 100-50-X	2	1.6	0.84
	189 100-50-T		1.0	0.53
	190 100-50-B		1.9	1.00
	191 100-90-X	1-	2.6	
Mesh 140 (d=1.24)	1 192 140-10-X	8-	10.5	0.97
	193 140-10-4		10.3	0.95
	194 140-10-3		10.4	0.96
	195 140-10-2		10.6	0.98
	196 140-10-1		10.8	1.00

Table 9 continued

Run number	Sample number	Bed thickness, mm	Percent of ilmenite	Separation ratio
Mesh 140 (cont'd)	197, 140-50-X	6	10.4	1.02
	198 140-50-T		10.5	1.03
	199 140-50-M		10.2	1.00
	200 140-50-B		10.2	1.00
	201 140-90-X	4-	10.4	1.02
	202 140-90-T		10.5	1.03
	203 140-90-B		10.2	1.00

Note ① The percent of ilmenite is expressed in weight %.
② Separation ratio: the relative amount of ilmenite found in one horizontal section compared to the amount found at the bottom of the core.
③ In the descriptive sample number, the first numeral refers to the run number; the numeral between the two dashes refers to the sampling site given in decimeters below the vertical partition; the last numeral identifies the sample in the core starting by 'one' at the bottom. T: top; M: middle; B: bottom; X: average.
- Sample no. 175 is void because it spattered on the hot plate.
④ minus (-) means slightly less.

Flow no. S-2 was the only one which displayed an almost pure quartz sand layer less than one mm-thick, near the top and right below the suspension-deposited layer of ilmenite. Sample no. 160 which displays this quartz-ilmenite banding, contained the same amount, 50% by weight, of both minerals.

Where the thickness of the turbidite at the upper end of the flume exceeded the thickness at the lower end by a factor of four or more

(see Tables 7 and 8), the amount of dense mineral found at the bottom of each core tended to vary markedly (by a factor of 2:1 to 10:1) along the length of the flume. Two generalizations can be made:

(1) Low density runs (up to 1.26) in which the sediments were easily put into suspension in the mixing box, formed the richest concentrations of ilmenite (up to 60%) of all the runs;

(2) Slurries in which the sediments were difficult to keep in suspension, either because of high densities or the lack of clay-sized particles in the runs having uniform grain sizes (mesh 100 and 140 as shown in table 8), displayed an impoverishment of dense minerals in the turbidite. The bulk of the ilmenite thus settled directly in the mixing box. Lateral and vertical grading were present in the runs S-3, 100 and 140 from coarse at the bottom to finer both at the top and in the down-flume direction. These gradations apply both to a diminution in the percentage of dense minerals and to grain size.

3. A model turbidity current

A flow with an initial density of 1.195 is chosen to model a turbidity current in nature. A density of 1.195 is about the maximum density allowed by several authors (see section III A.3) and yields a turbidite thick enough to be sampled.

The depth of the underflow in the model is about 10 cm, whereas in nature it would be in the order of meters (see table 4). A length scale of 1/100 is thus employed. Since the length of the large flume starting at the vertical partition is 2 meters, that of the prototype would be a little more than 200 meters long because the flow is unhindered by a wall

in the down-current direction.

Froude similarly requires that the velocity of the current in the model be reduced to 1/10 of the velocity in the prototype (section III D.1). Since the velocity of the runs having an initial density of 1.195 is about 20 cm/sec (experiments nos. 3, A and B) the prototype would then flow at a velocity of 200 cm/sec.

In experiments A and B the settling velocity of both ilmenite and quartz was 1.5 cm/sec corresponding to an average grain diameter of .150 mm for the quartz grains. The ilmenite had a mesh size (+200 -140) corresponding to grain diameters of .076 mm to .105 mm. The determination of settling velocity was treated in section IV A.2. The average fall velocity of the quartz grains in the prototype would be 15 cm/sec. However, the effective settling velocity of the particles would be less than the above values because the grains actually settle through a suspension (hindered settling) and not in clear water (Middleton, 1966c).

Table 10 shows the ratio of settling velocity to average velocity, w/u, and the Froude number encountered in natural turbidity currents and in model experiments.

Table 10

w/u ratios and Fr values for turbidity currents

	$\frac{w \text{ cm/sec}}{u \text{ cm/sec}}$			Froude Number Fr
nature, average (1)	2/1000	=	2×10^{-4}	.2 to 3.0
model, Middleton 1965	.9/30	=	300×10^{-4}	.7
model, expt A,B	1.5/20	=	750×10^{-4}	.5
protype for A	15/200	=	750×10^{-4}	.5

(1) A median diameter of .180 mm is taken to calculate w. The range of Froude numbers and velocities encountered in turbidity currents was given in table 4.

Experiment A had the same density, 1.195, and proportion of quartz to ilmenite, 5:1, as experiment 3, but the grain size of the ilmenite was slightly larger in experiment A. This caused a decrease in velocity of about 1 cm/sec (table 6) in experiment A thus lowering slightly the Froude and Reynold's numbers (table 9). The total resistance to the flow, f, increased with decreasing Re and Fr values. This may be accounted for by the fact that quartz occupies more space per unit weight than ilmenite. The volume concentration of the particles in the initial slurry is thus increased and causes more collisions between the particles, thus decreasing the velocity of the turbidity current and increasing the resistance to the flow from the walls and upper interface.

Thick sections of experiment A were made by impregnating the turbidite with resin. Samples were taken at 2, 7, 12 and 17 dm down-flume.

The ilmenite-rich layer that covered the upper part of the turbidite is shown in plate 3. This ilmenite-rich layer was found in all the runs in this thesis, irrespective of the density of the initial slurry. The layer was mainly deposited from the sediment remaining in suspension, once the turbidity current had flowed through the length of the flume. The middle of the turbidite, 7 dm down-flume, displayed a relative impoverishment in ilmenite (plate 4) compared to the other sections farther down-flume. The turbidite displayed lateral and vertical grading in the size of the quartz grains from coarse at the bottom and up-flume to fine at the top and down current (plate 5). Grading of the ilmenite grains was hardly noticeable because of its restricted range in grain size.

Plate 3

Ilmenite (white) concentration on top of turbidite in mixing box; quartz grains (grey) display vertical grading. Reflected light, X 16.

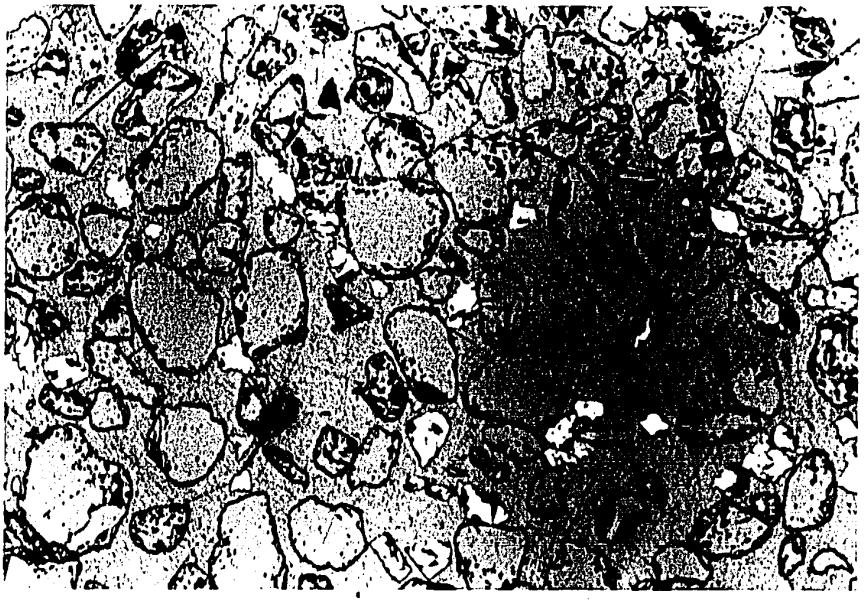

Plate 4

Middle of turbidite deposited 7 dm from the gate. Reflected light, X 16.

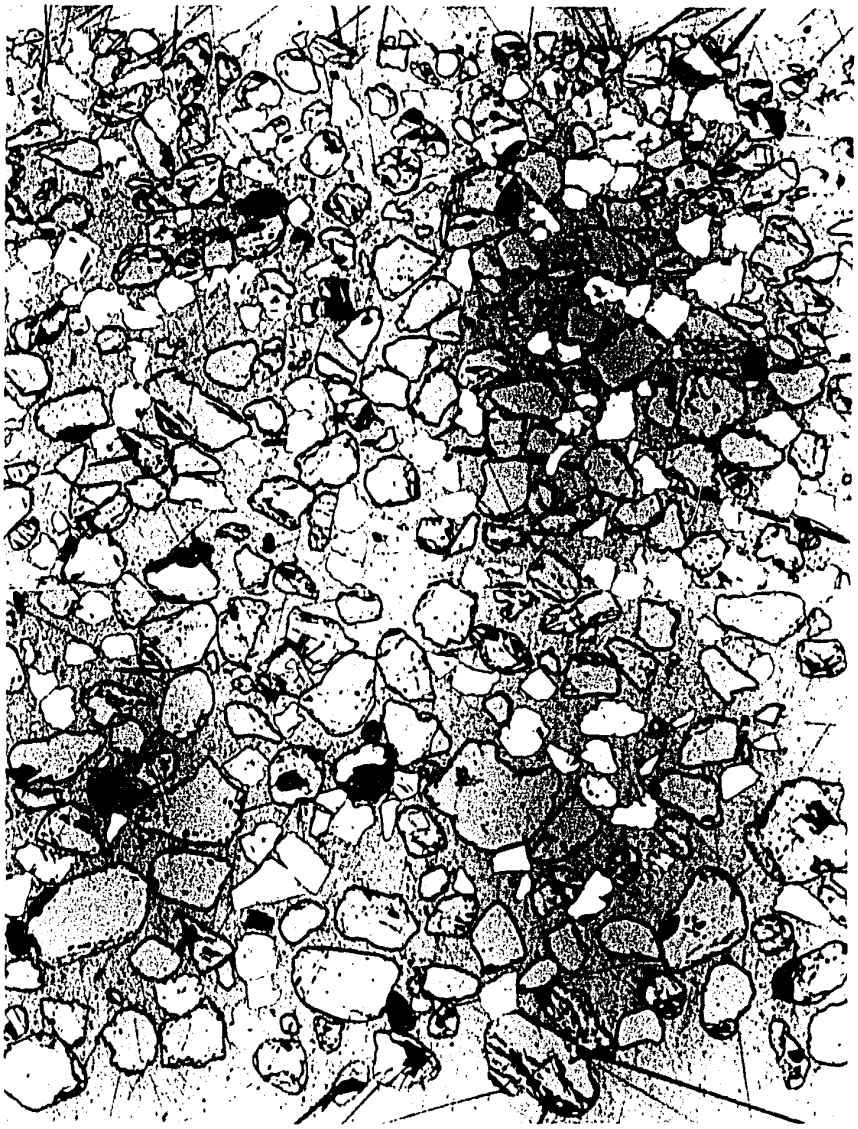

Plate 5

Vertical size grading of ilmenite (white) and quartz (grey) going upwards; 17 dm from the gate. Reflected light, X 16.

Experiment B had the same density and grain diameters as experiment A, but the proportion of quartz to ilmenite was greater, 9:1. Since the volume concentration of the particles in the suspension was greater, because of the greater amount of quartz, more collisions between the particles occurred. The total resistance to the flow increased slightly (table 9). Its velocity was 15% lower than the velocity of experiment A (table 6). The Froude and Reynold's numbers were thus smaller for experiment B.

Experiments A and B modelled a turbidity current of modest size such as could be generated by a slump which has the order of magnitude of the slumps (50 m X 50 m) found in the Kuroko-type ore deposits (last field example treated in this thesis). Some slumps, that generate turbidity currents in submarine canyons are of an entirely different order of magnitude: they cover an area of millions of square meters (Menard, 1964).

In order to model longer turbidity currents, a further reduction in the settling velocity of the particles would be necessary. This could be achieved partly by further scaling-down the diameters of the particles and by choosing particles which have a lower density.

CHAPTER V

Field Examples

A. MUFULIRA OREBODIES, ZAMBIA (N. RHODESIA)

Introduction

The Mufulira orebodies are situated in the northernmost part of the Copperbelt in Zambia in the vicinity of latitude 13° south and longitude 28° east (see insert of figure 8). The Copperbelt is a rectangular strip of country trending in a northwestern direction. It is about 30 miles wide, adjacent to the Congo border, marked by the watershed between the Congo and Zambesi river drainage systems, and stretches for about 100 miles from Honkola in the northwest to Roan Antelope and Bwana Mkubwa in the southeast (Mendelsohn, 1961, p. 1).

1. General geology.

The rocks of the Copperbelt are divided into the Katanga system and the Basement complex (table 11). The Basement of early pre-Cambrian age has fairly widespread mineralization but of no economic importance. The overlying Lower Roan group belonging to the Katanga system of late pre-Cambrian or Cambrian age contains all the copper deposits of the Copperbelt (Mendelsohn, 1962, p. 61). The deposits consist of disseminated sulfides in sedimentary formations. The sulphides generally make up 5 to 15% of the rock by weight. The grain size of the sulphides and of the host rock generally increase together. The main sulphides are pyrite, chalcopyrite,

Table 11

Stratigraphic column of the Katanga System, Zambia
(after Mendelsohn, 1961).

GABBRO-Intrusive, commonly into the Upper Roan dolomites

Series	Group	Formation	Rock Types (Minor or rare rock types in parentheses)
KUNDELUNGU	UPPER	---	Shale, quartzite
	MIDDLE	---	Shale Tillite
	LOWER	KAKONTWE	Shale
		TILLITE	Dolomite and shale Tillite
MINE	MWASHIA	---	Carbonaceous shale, argillite (dolomite and quartzite)
	UPPER ROAN	---	Dolomite and argillite (quartzite, breccia)
		---	Argillite and quartzite
	LOWER ROAN	HANGINGWALL	Quartzite Argillite, and feldspathic quartzite (dolomite)
		ORE	Argillite, impure dolomite, micaceous quartzite (graywacke, arkose)
		FOOTWALL	(Footwall conglomerate) Argillaceous quartzite Feldspathic quartzite Aeolian quartzite Conglomerates

UNCONFORMITY

BASEMENT COMPLEX-ancient Precambrian schists intruded by granite.

bornite, and chalcocite. The lower formation of the Lower Roan group consist of conglomerate and quartzites. The western part of the ore formation is made up of impure dolomite overlain by argillite, known as ore shale, and underlying footwall conglomerate. In the Mufulira syncline the ore formation consists of quartzites with some carbonaceous quartzites, or graywacke, dolomite and argillite. The hanging-wall formation mainly consist of quartzites, arkoses and shales.

2. Mufulira 'A', 'B' and 'C' orebodies.

The Mufulira orebodies consist of three superimposed copper sulfides deposits, each having in its midst a lenticular graywacke body which was deposited by turbidity currents (Garlick, 1967). A NW-SE section is shown in figure 8. The dimensions of the orebodies and the copper-bearing minerals are shown in table 12.

TABLE 12

Dimensions of the Mufulira Orebodies

Orebody	Proved Strike Lth.	Average Thickness	Dominant Copper Minerals	Present P.C.
A	6,000 ft.	20 ft.	chalcocite	10%
B	10,500 ft.	25 ft.	bornite	3%
C	18,000 ft.	45 ft.	chalcopyrite	3%

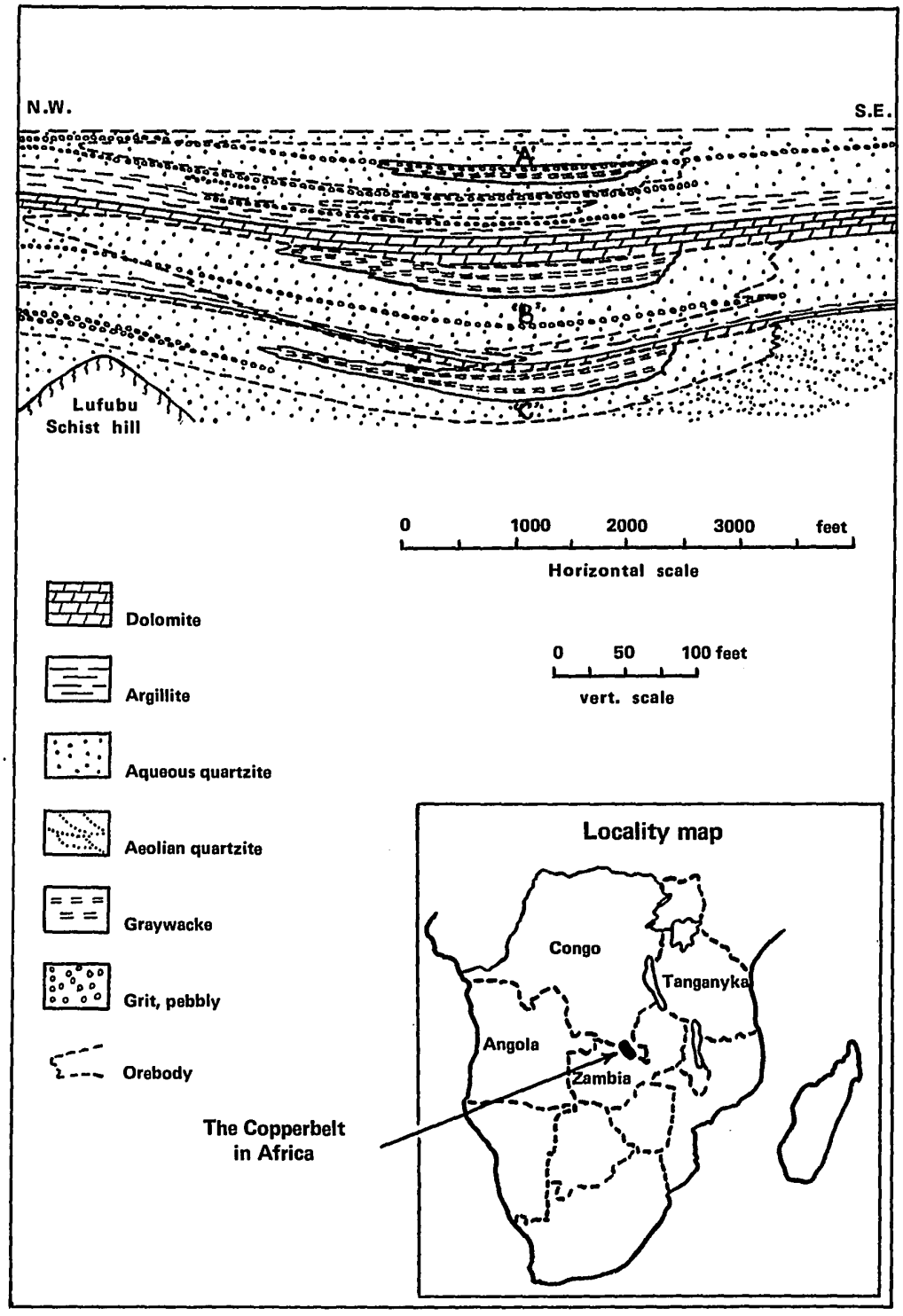

Figure 8. The Mufulira 'A', 'B' and 'C' orebodies; Zambia (after Garlick, 1967)

The Mufulira 'C' orebody, which is the lowest stratigraphically, is 18,000 feet long, 5000 feet at its smallest width and has an average thickness of 45 feet. According to Garlick (Mendelsohn, 1962), at its narrowest width, it contains a narrow zone of disseminated pyrite in the centre of the basin with copper sulfides on both sides. The pyritic zone widens northwards. The sulfides are zonally arranged about a pyritic core: pyrite is found at the center then chalcopyrite and finally bornite furthest out. In the ore-shale type deposits cross-bedding and changes of facies indicate that currents flowed mainly from northeast to southwest, that is, from the higher lands on the northeastern side of the Mufulira geosyncline southwest towards the centre of the geosyncline. Garlick (1967) shows the relations of sulfide precipitation and mineral zones to the detrital facies in an idealized diagram (figure 9). The sedimentary features found on the western shoreline are repeated on the eastern side of the deposit.

According to Garlick (in Mendelsohn, 1962), the western edge of the deposit starts with crossbedded barren feldspathic quartzite and, following the direction of the old currents, the orebody begins with disseminated bornite. Further down-current, chalcopyrite appears and increases as the bedding becomes crumpled as both the sulfide and mud content increases. Slumping of the sediments produced a slump breccia with bornite and chalcopyrite dissemination. Several barren wash-outs (minor river channels) are found within the slump breccia. This part of the deposit corresponds to the proximal facies of the turbidite. Farther out in the basin, turbidity currents developed and deposited other grey quartzites

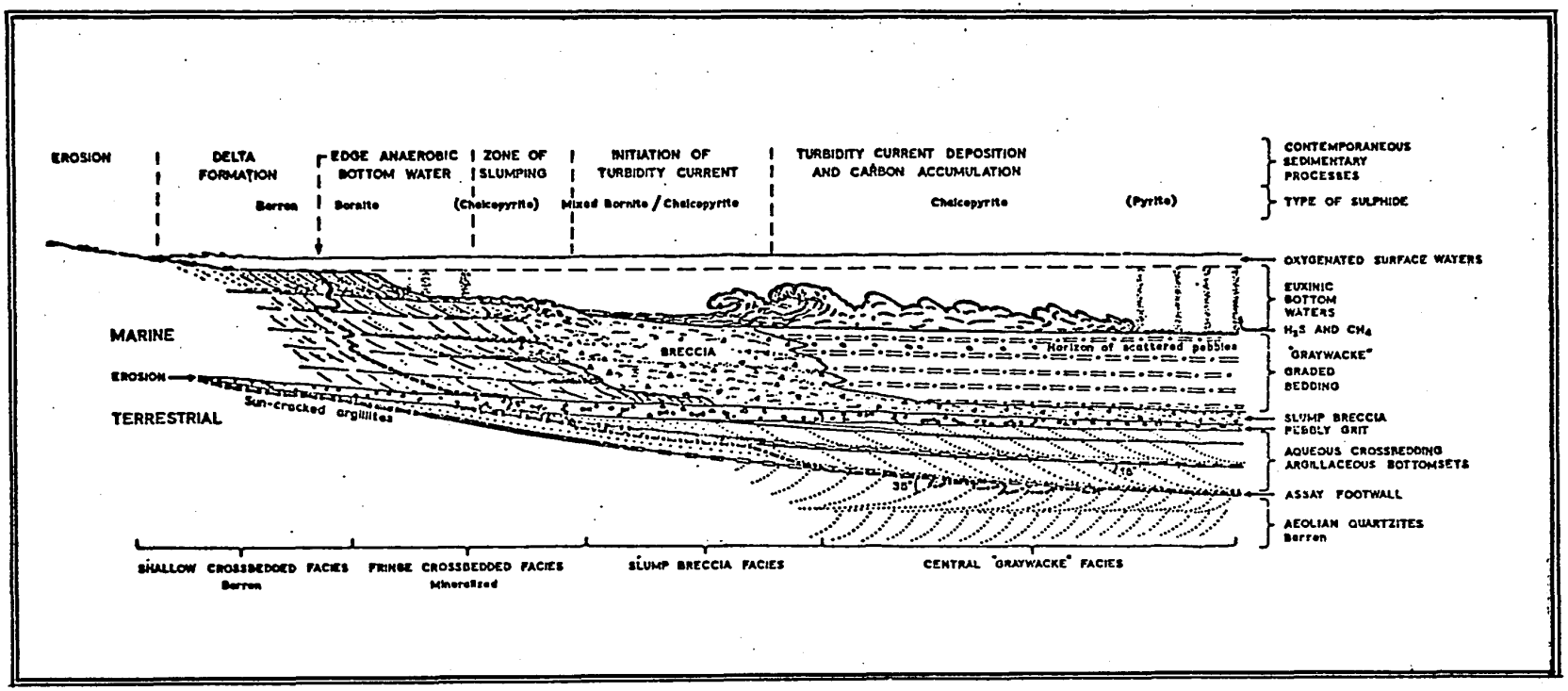

Figure 9. Relation of sulphide precipitation and mineral zones to detrital facies of Mufulira type orebodies. (from figure 30 in Garlick, 1967).

with disseminated sulphides, mainly chalcopyrite. Finally greywacke containing chalcopyrite and pyrite was deposited at the center of the basin. The greywacke is a carbonaceous argillaceous quartzite and corresponds to the distal facies of the turbidite. The carbonaceous material occurs only in the greywackes, as small granules in the matrix and as graphitic fluid on detrital grain surfaces (Brandt et al. 1961). The same features are repeated in the overlying 'B' and 'A' orebodies.

The quartzites have well defined heavy mineral concentrations, particularly on the truncation surfaces of the cross-bedding (Mendelsohn, 1962).

The greywacke which is considered to be a local facies of the underlying grey sericitic quartzite is medium-grained with a maximum diameter of one millimeter. The bases of the orebodies are generally well-bedded. The size of the sulfide grains is a function of recrystallization. The greywacke is not recrystallized; it carries fine sulfides in its matrix. Contrary to the other deposits in the Copperbelt, there is no relation at Mufulira between the grain size of the sediments and that of the sulfide mineral grains.

According to Garlick, "There are far greater amounts of sulphur locked up in the sulphates of the Lower and Upper Roan than there is as sulphides, and this indicates that in this region where Lower and Upper Roan were deposited there was no deficiency of sulphur and that the anaerobic bacteria would have plenty of sulphate material from which to produce hydrogen sulphide for the precipitation of the metals (in

Mendelsohn, 1961, p. 18). Anhydrite occurs within the dolomites of the Upper Roan and as large crystals associated with and replaced by carbonate in the ore formation.

3. Mineralogy

Table 13 shows the mineralogy of the greywacke which occurs in the upper and middle horizons of the 'B' and 'C' orebodies.

TABLE 13

Mineralogy of the ore-bearing greywackes (after Brandt et al., 1961, pp. 446-447).

	Average Percentages of Minerals by Volume	
Minerals	"B" Upper and Middle Horizon	"C" Upper and Middle Horizon
Quartz	65	70
Fresh feldspar	5	5
(mostly microcline)	10	5
Sericite-Quartz pseudomorphs	10	5
Muscovite	5	5
Interstitial sericite	10	5
Carbonates (mostly dolomite)	5	5
Carbonaceous material	5	5
Copper sulphides	5	9

4. Ore Genesis

The orebodies are associated with sedimentary features, and are unrelated to any known igneous or tectonic activity. The sulfides are syngenetic with the host rocks. Pre-consolidation slumping on the margins of the deposit may have caused some thinning and minor disturbance of the mineralization. The initiation of turbidity currents further downslope could explain the thickness of ore found in the central part of the basins within the greywackes.

The general distribution of the sulfide minerals has been explained by the zonal theory of selective precipitation of Garlick (in Mendelsohn, 1961). According to the zonal theory only barren sediments with very little diagenetic pyrite are deposited in the oxygenated waters near shore. In slightly deeper waters the production of hydrogen sulfide by anaerobic bacteria precipitated much copper and a small amount of iron. Farther offshore copper and iron sulphides are precipitated in equal amounts. In the interior of the basin, copper is depleted and iron sulphide is the dominant precipitate.

The metals may have been precipitated as fine, colloidal, mixed sulfides or hydroxides. The minerals chalcocite, bornite, chalcopyrite and pyrite were formed by later diagenetic and metamorphic processes.

Experiments have been made by the Metallurgical Research Laboratory of R.S.T. Mine Services Ltd. to simulate the selective precipitation of sulfides (Mendelsohn, 1962). The zonal principle works in practice. Garlick (in Mendelsohn, 1961, p. 154) writes that: "... at Mufulira West

copper sulphides are anticipated and usually found between the pyritic dissemination in the centre of the basin and the barren, shallow water sediments at the edge of the basin. Recently, geologists of the Union Minière discovered the same zonal arrangement on a large scale in the Kolwesi district."

The coarser pebbles at the bottom of each turbidite were deposited from a suspension, because the more spherical particles are found on the same horizon as the larger less spherical particles.[1]

By taking 3 cm as the diameter of the large grain at the bottom of the turbidite and 2.7 and 1.2 as the respective densities of the grain and the turbidity current, the threshold stress, τ_{to}, and the flow velocity, $\bar{u}$, of the turbidity current would be respectively, 265 dynes/cm_2 and 250 cm/sec (9 km/hr).[2]

The sudden, sporadic releases of the turbidity flows probably gave rise to vertical grading in the greywacke. Otherwise, if the flows were fed for some time at a constant rate, non-graded greywacke would have formed.[3]

B. THE NAIRNE PYRITIC FORMATION, AUSTRALIA

Introduction

According to Skinner (1958) the Nairne Pyritic Formation is composed of several sulfide-bearing members separated by sulphide-free greywackes, at the base of the Kanmantoo Group believed to be Cambrian in age. The Kanmantoo rocks outcrop at the eastern side of the Mt Lofty Ranges,

---

1. cf page 16
2. cf page 17
3. cf page 24

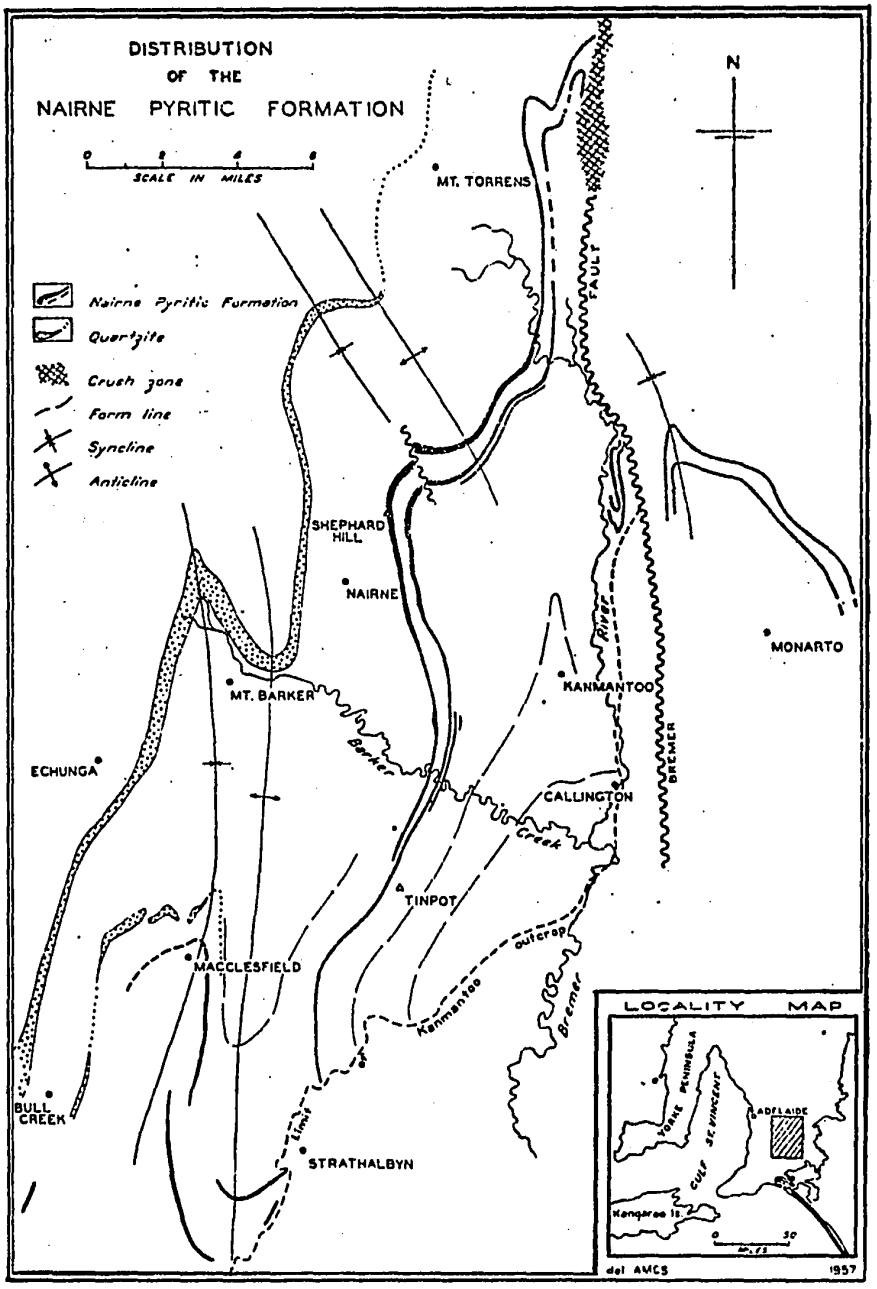

Figure 10. The Nairne Pyritic Horizon, South Australia (from Figure 1 in Skinner, 1958).

South Australia (see figure 10). This Group has been regionally metamorphosed and consists of 26,000 feet of greywacke, quartzite and siltstone which display small scale cross-bedding, poor graded bedding and sedimentary slump structures. The pyritic beds outcrop for a distance of at least 65 miles and locally at Nairne it thickens, and the beds dip approximately 70°E and strike generally N-S (Thomson, 1965).

1. Primary and secondary pyrite.

Ninety per cent of the pyrite in the formation is considered primary, that is, it occurs as small grains (2mm and less) parallel to the bedding and also in small tension gashes. Good crystal outlines exist where pyrite and pyrrhotite are in contact; whereas, where pyrite is in contact with the gangue, poor crystal outlines prevail. Two varieties of secondary pyrite are accounted by pyrrhotite alteration: (i) concentric pyrite which consists of pyrite, marcasite, or pyrite and marcasite; (ii) zoned pyrite which may be either a direct replacement of pyrrhotite or a replacement of the concentric pyrite. Less than .1 per cent of the pyrite in the ore formation was deposited by circulating ground water and is found in small cracks in the weathered portion of the works (La Ganza, 1959).

2. Sulphide-bearing members

Each sulphide-bearing member is composed of many thin-bedded, sulphide-bearing greywackes and siltstones ranging from one inch to ten feet in thickness. The sulphides are represented by roughly equal amounts of pyrite and pyrrhotite which together average about 10% by volume (16.5% by weight) of each member. Minor amounts of sphalerite and chalcopyrite

and traces of arsenopyrite are also present. The sulphide-bearing members are always conformable. Where the beds pinch out, the rocks are finer grained and show a decrease in sulphide content with an increase in muscovite.

About 5 per cent of the beds show grading with a range in grain size from 0.03 mm to 0.2 mm. This could indicate that a constant supply of sediments was available (Kuenen and Menard, 1952, p. 88).

Skinner (1958, p. 550) notes that the sulphides have the same grain size as the silicates, being coarse in the coarse sediments and fine in the fine-grained sediments. This is more readily seen in graded units. Pyrite also tends to be concentrated at the base of graded beds.

3. Metamorphism

Although individual beds may be classified as quartzites, greywackes or siltstones, the mineralogy is limited to a few assemblages. According to Skinner (1958, p. 546) : "64 percent of the host rock is a quartz-muscovite-albite-microcline assemblage. 25 to 30 percent is a quartz-muscovite-albite (andalusite, kyanite) assemblage. The remainder occurring in beds less than 1 foot thick, is a quartz-biotite-albite-microcline, quartz-muscovite-scapolite-plagioclase or quartz-biotite-spessartite-feldspar assemblages."

Pyrite alters to pyrrhotite after a certain stage in metamorphism. Scott and Barnes' (1971) analysis of sphalerite-pyrite-pyrrhotite assemblages from Nairne, found sphalerite to contain 15.2 mole per cent FeS. Sphalerite used as a geobarometer indicates a pressure of 2 1/2 kilobars,

at the Sheppard Hill Quarry. The pressure can usually be estimated within ± 1 kilobar (Scott and Barnes, 1971). For comparison, the co-existing kyanite and andalusite which, according to Skinner, appear to have grown as an equilibrium pair indicate a pressure of 2.2. kilobars (from the data of Richardson, Gilbert and Bell, 1969).

4. Ore genesis

The sulphide-bearing members are always conformable. Where the beds pinch out, the rocks are finer grained and show a decrease in sulphide content with an increase in muscovite. This could indicate the directions of the turbidity currents which deposited the greywacke. The heavy mineral concentration in bands in the coarser rocks and at the base of graded beds suggests the original iron sulfides were deposited as detrital grains and not chemically precipitated in situ. A syngenetic theory involving the redeposition of iron sulfides in deep water by turbidity currents would be in accord with the field observations. Later metamorphism would change the original sulfides to the assemblages observed today.

The redistribution of heavy mineral by turbidity currents should be retained in a multiple working hypothesis approach (Ellison, 1960) in the search for sulphides in greywacke rocks.

C. THE NO. 1 KUROKO DEPOSIT OF THE SHAKANAI MINE, JAPAN

Introduction

Strata-bound base metal sulphide deposits of Miocene age in Japan are known as the Kuroko ore deposits (Kajiwara, 1970). They are almost always associated with gypsum deposits and acidic volcanic rocks. The no. 1

deposit of the Shakanai mine is composed of sulfide ore and gypsum ore. Kajiwara (1970) subdivides the metallic ores as follows:

Syngenetic ores	Epigenetic ores
a) massive ore	a) disseminated ore
b) fragmental ore	b) veins and stockworks

The writer will consider only syngenetic fragmental ore because they support the idea of submarine slumping or sliding as will be shown below. These in turn are believed to be the main processes that give rise to turbidity currents.

1. Fragmental ore.

The fragmental ore is composed of ore fragments associated with minor lithic fragments. It is essentially a clastic equivalent of the massive ore: The fragmental ore is subdivided into three categories by Kajiwara (1970, p. 199):

a) Kuroko (black ore): sphalerite, galena, tetrahedrites, barite, chalcopyrite, and pyrite with minor amounts of accessory minerals.

b) Oko (yellow ore): chalcopyrite and pyrite.

c) Ryukako (pyrite ore): pyrite.

The fragmental structures within the geologic profile of the no. 1 deposit is illustrated in figure 11. A close-up of a graded ore-bed is illustrated in figure 12.

The sedimentary features of the ores are:

1. Graded bedding of ore fragments (lateral and vertical size-grading of ore fragments.)

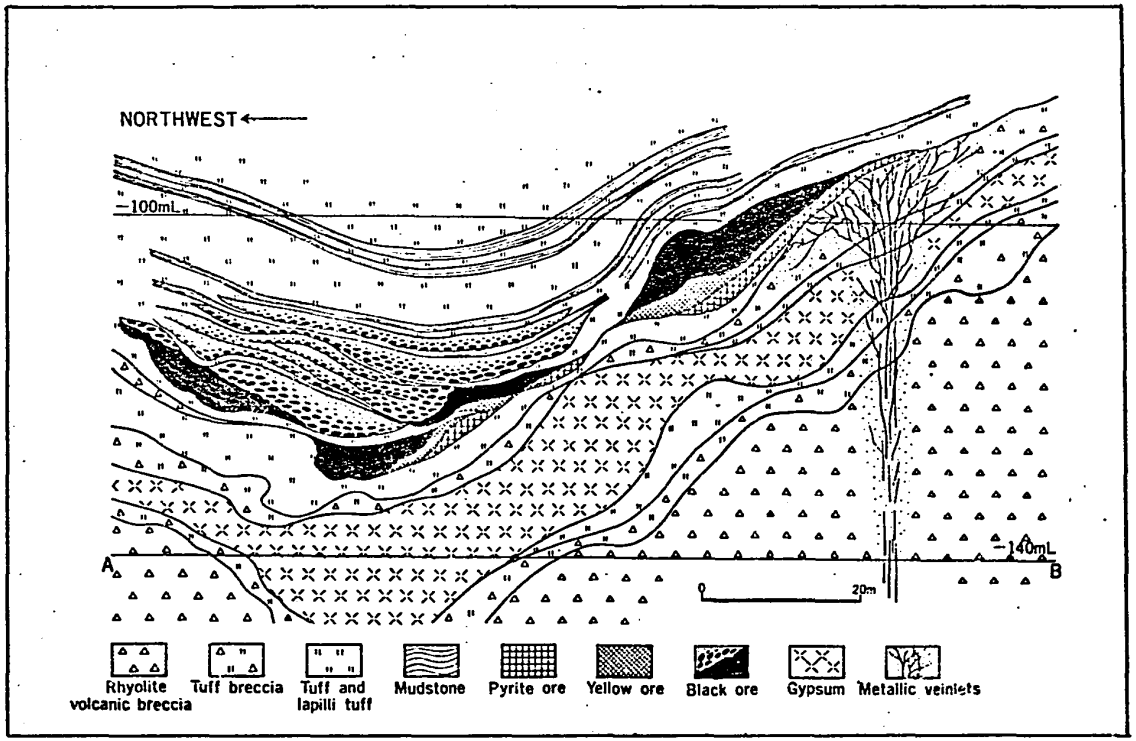

Figure 11. Geologic profile of No.1 ore deposit of the Shakanai mine, Japan (reproduced with permission of T.Tatsumi, Ed.).

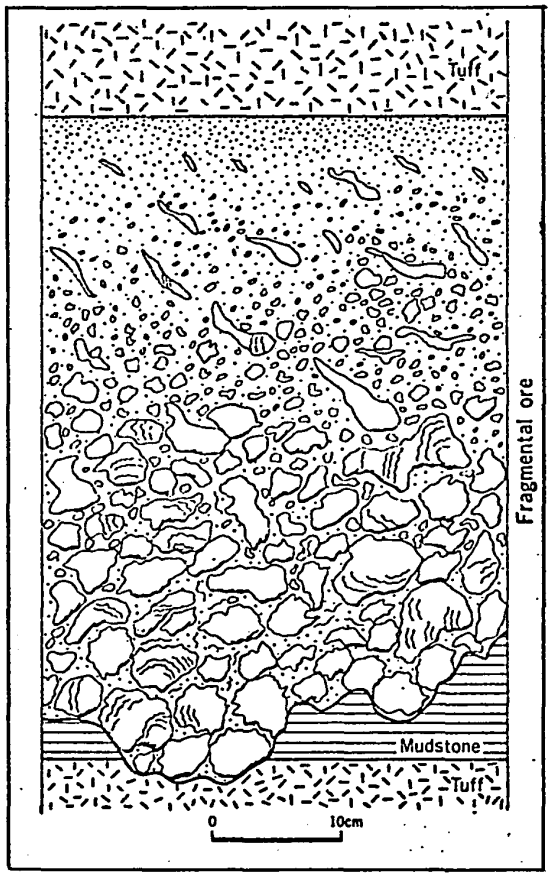

Figure 12. Typical mode of occurrence of a thin graded ore bed.

2. A channeling or grooving structure at the bottom of each graded ore bed.

3. An imbricate structure of platy ore fragments within each graded ore bed.

4. Cross lamination of fine ore fragments at the uppermost part of a graded ore bed.

5. Latteral facies change, from massive ore to fragmented ore (massive → blocky → breccia → powdery), in an orebody (Kajiwara, 1970, p. 205).

2. Genesis

Dr. T. Tatsumi (personal communication) suggests the following processes of formation for the Kuroko ore deposits.

1. Feeder channels (as shown in the geologic profile of figure 11) within the silicified zone provided the ascending hot mineralized fluid.

2. Chemical precipitation in the sea gave rise to the massive ore.

3. Sliding and slumping of the massive ore gave rise to the fragmental ore.

3. Application.

Kuroko ore deposits, relatively small in plan (50m x 50m), are found between rhyolite domes. Were there no barriers to end the slumping, turbidity currents might have developed. It is suggested that a mineralized turbidite, even if it is 'uneconomic', should be analyzed to find its up-flow direction. A mineralized turbidite (which covers a large area) could be used as an guide to ore-finding, since the Kuroko ore

deposits are relatively small in plan. The general geology of the area and the nature of the intervening rocks between the turbidites offer clues to the origin and possible extent of the turbidite. For example, if the turbidite is situated in front of an ancient delta, it was probably generated by slumping of the sediments on the deltaic front. If the turbidite is surrounded by volcanic domes, it could have been triggered by submarine volcanic explosions.

Summary and Conclusions

Turbidity currents can re-distribute dense minerals which were previously precipitated or transported in shallower water.

The two major pyritic members of the Nairne Pyritic Formation in Australia outcrop over a distance of at least 65 miles. The 'C' orebody horizon of the Mufulira orebodies in Zambia has a total strike length of 11 miles. In both deposits the sulfides occur mostly in greywackes and frequently show grading in particle size. The size of the slumps found in the no. 1 Kuroko deposit of the Shakanai mine in Japan could produce the prototype-turbidites which have been modelled in this study.

The density of the turbidity currents in nature may reach a maximum of 1.20; whereas, in experimental studies densities as high as 2.00 and over have been used in the initial slurries.

In flume experiments, runs may attain a velocity of 1m/sec. In nature a maximum of 20 m/sec has been calculated. In the present experiments, there is a good correlation between increasing velocities and increasing densities given by the formula;

$$\log_{10} u = -1.67 + 1.71 \log_{10} \sqrt{\frac{\Delta\rho}{\rho_t} \times g \times H}$$

The rate of increase in the velocity of the turbidity current decreases as the density of the initial flow increases.

When the density of the initial suspension is kept constant, a greater amount of coarser material in the initial flow will increase the total

resistance to the flow thereby decreasing the velocity of the turbidity current. The Froude and Reynold's numbers will thus be diminished.

Clumps of grains, mineral banding and waves at the upper bed surface have been found in only a few of the present experiments.

Vertical grading was seen more easily in the smaller flume, especially when the dense mineral was sphalerite rather than ilmenite. According to Middleton (1967) a sudden release of the slurry produces (1) both normal and lateral grading with low concentration flows and (2) 'coarse tail' vertical grading with lateral grading at the bottom with high concentration flows. When the slurry is fed at a regular rate for some time no grading occurs.

The turbidites tapered markedly downflume in the two following sets of flow conditions which produced contrasting results:

(1) Low density runs (up to 1.26) in which the slurries were easily put into suspension formed the richest concentrations of dense minerals;

(2) Slurries in which the sediments were hard to keep in suspension displayed an impoverishment of heavy minerals in the turbidite. The relative enrichment took place in the mixing box. It would therefore be useful while prospecting to search 'upstream' of the sulfide bearing greywackes in order to find a possible enriched zone of slumping. Vertical grading is better developed in the zone of slumping than in the ensuing turbidite, both in these experiments and in nature. This vertical grading is well displayed in the no. 1 deposit of the Shakanai Mine in Japan (Kajiwara, 1970).

Claims to original work

The purpose of this thesis was to investigate the behaviour of heavy minerals carried within a turbidity current. Although a fair number of experiments have been done on small-scale turbidity currents, this is the first attempt to simulate sulfide-bearing turbidity currents. This work was done primarily by using fixed ratios of dense to lighter minerals over a wide range of densities and by varying the settling velocity of ilmenite.

The following original results were noted:

(1) Low density runs (up to 1.26) in which the sediments were easily put into suspension in the mixing box formed the richest concentrations of ilmenite.

(2) Slurries in which the sediments were difficult to keep in suspension, either because of high densities or the lack of clay-sized particles in the runs displayed an impoverishment of dense minerals in the turbidite.

(3) When the density of the initial suspension is kept constant, a greater amount of coarser material in the initial flow increases the total resistance to the flow thereby decreasing the velocity of the turbidity current. The Froude and Reynold's numbers will thus be diminished.

Suggestions for further work

A further step in simulating natural turbidites would be achieved by accumulating sediments on a very gentle slope of a flume either through precipitation or transportation until the sediments become unstable and begin to slide down the slope. This would in turn initiate the turbidity flow in a more natural fashion.

Although the density or rather the variation in density of the initial sediment-water slurry would be difficult to appraise, closer correlations between natural and experimental turbidites would be achieved.

In order to model longer turbidity currents, a further reduction in the settling velocity of the particles would be required. This could be partly achieved by further scaling-down of the diameters of the particles and by choosing particles with low density.

Acknowledgements

The author wishes to thank Professor L. A. Clark[1] formerly of McGill University for suggesting this problem and for his advice during part of this study. Thanks are extended to Dr. W. H. MacLean of McGill University for his guidance and review of the manuscript.

1. Dr. L. A. Clark is now at the service of Kennecott Exploration Inc., Salt Lake City, Utah.

BIBLIOGRAPHY

ALLEN, J. R. L. 1971. Mixing at turbidity current heads, and its geological implications. J. Sediment. Petrol., 41, pp. 97-113.

AMSTUTZ, G. C. and BUBENICEK, L. 1967. Diagenesis in sedimentary mineral deposits. In Developments in sedimentology, 8 (G. Larsen and G.V. Chilingar, Ed,). Elsevier, Amsterdam, pp. 417-475.

BAGNOLD, R.A. 1962. Auto-suspension of transported sediment; turbidity currents. Roy. Soc. London, Proc., ser. A, 265, pp. 315-319.

BELL, H.S. 1942. Density currents as agents for transporting sediments. J. Geol., 50, pp. 512-547.

BENJAMIN, T.BB. 1968. Gravity currents and related phenomena. J. Fluid Mechanics, 31, part 2, pp. 209-248.

BRANDT, R. T., BURTON, C. C. J., MAREE, S.C. and WOAKES, M.E. 1961. Mufulira. In The geology of the Northern Rhodesia Copperbelt (F. Mendelsohn, Ed.). Macdonald, London, pp. 411-461.

BRUSH, L. M., Jr. 1965. Sediment sorting in alluvial channels. In Primary sedimentary structures and their hydrodynamic interpretation (G.V. Middleton, Ed.). Symposium Soc. Econ. Paleon. Miner., Tulsa, Okla., pp. 25-33.

BULLARD, Sir Edward. 1969. The origin of the oceans. Scientific Amer., 221, pp. 66-75.

COLBY, B. R. and SCOTT, C. H. 1965. Effects of water temperature on the discharge of bed material. In Sediment transport in alluvial channels. U.S. Geol. Surv., Prof. Papers 462-G, p. 25.

DORSEY, E. N. 1940. Properties of ordinary water-substance. A compilation. Reinhold Publishing Corp., New York, p. 673.

DZULINSKI, S. W. 1965. New data on experimental production of sedimentary structures. J. Sediment. Petr., 35, pp. 196-212.

DZULINSKI, S. W. and WALTON, E. K. 1965. Sedimentary features of flysch and greywackes. In Developments in sedimentology, 7, Elsevier, Amsterdam, p. 274.

EL BAZ, F. and AMSTUTZ, G. C. 1964. Generations of diagenetic crystallization in the Cu-Pb-Co-Ni deposit of Frederickton, Missouri. In Developments in sedimentology, 2 (G.C. Amstutz, Ed.). Elsevier, Amsterdam, pp. 73-75.

ELLISON, S. P. 1960. Thinking patterns for geologists. Bull. Am. Assoc. Petrol. Geol., 44, p. 980.

EMERY, K. O. 1969. The continental shelves. Scientific Amer., 221,pp. 107-122.

FISHER, R. V. and WATERS, A. C. 1969. Bed forms in base-surge deposits: lunar implications. Science, 165, pp. 1349-1352.

———1970. Base-surge bed forms in maar volcanoes. Am. J. Sci., 268, pp. 157-180.

GARLICK, W.J. 1967. Special features and sedimentary facies of stratiform sulphide deposits in arenites, Zambia, In Sedimentary ores. 15th Inter-University Geol. Cong., University of Leicester, England, pp. 107-169.

GILES, R. V. 1962. Schaum's outline of theory and problems of fluid mechanics and hydraulics, 2 ed., McGraw-Hill, New York, p. 274.

HURLEY, R. J. 1964. An analysis of flow in Cascadia deep-sea channel. In Papers in marine geology (R.L. Miller, Ed.). The Macmillan Co., New York, pp. 117-132.

JACKSON, K. C. 1970. Textbook of lithology. McGraw-Hill, New York, p. 673.

JOPLING, A. V. 1965. Laboratory study of the distribution of grain sizes in cross-bedded deposits. In Primary sedimentary structures and their hydrodynamic interpretation (G.V. Middleton, Ed.). Symposium Soc. Ec. Paleon. Miner., Tulsa, Okla., pp. 53-65.

KAJIWARA, Y. 1970. Syngenetic features of the Kuroko Ore from the Sha-Kanai Mine. In Volcanism and ore genesis (T. Tatsumi, Ed.). University of Tokyo Press, pp. 197-206.

KEEN, M. J. 1968. An introduction to marine geology. Pergamon Press, New York, pp. 218.

KOMAR, P. D. 1970. The competence of turbidity current flow. Bull. Geol. Soc. Amer., 81, pp. 1555-1562.

KRAUME, E. 1955. Die Lagerstatte des Rammelsberges bei Goslar (English summary). Hannover, pp. 352-353.

KUENEN, Ph. H. and MIGLIORINI, C. I. 1950. Turbidity currents as a cause of graded bedding, J. Geol., 58, pp. 91-127.

KUENEN, Ph. H. and MENARD, H. W. 1952. Turbidity currents, graded and non-graded deposits, J. Sediment. Petrol., 22, pp. 83-96.

KUENEN, Ph. H. 1957. Sole markings of graded graywacke beds. J. Geol., 65, p. 237.

LaGANZA, R. F. 1959. Pyrite investigations at Nairne, South Australia. Econ. Geol., 54, pp. 895-902.

MENARD, H. W. 1964. Marine geology of the Pacific. McGraw-Hill, New York, p. 271.

———1969. The deep ocean floor. Scientific Amer., 221, pp. 127-142.

MENDELSOHN, F., Editor, 1961. The geology of the Northern Rhodesian Copperbelt. Macdonald, London, p. 523.

———1962. The geology of the Northern Rhodesian Copperbelt. In Seventh Tech. Proc. of the Northern Rhodesia Section of the Commonwealth Mining and Metallurgical Congress of 1961, pp. 5-30.

MIDDLETON, G. V. 1962. Size and sphericity of quartz grains in two turbidite formations. J. Sediment. Petrol., 32, p. 725.

———1965. Experiments on turbidity currents. Tech. Memo 65-9, California Institute of Technology, p. 12.

MIDDLETON, G. V. and BRIGGS, L. I. 1965. Hydromechanical principles of sediment structure formation. In Primary sedimentary structures and their hydrodynamic interpretation (G.V. Middleton, Ed.). Symposium Soc. Ec. Paleon. Miner., Tulsa, Okla., pp. 5-16.

MIDDLETON, G. V. 1966a. Experiments on density and turbidity currents. I Motion of the head. Can. J. Earth Sci., 3, pp. 475-546.

———1966b. Experiments on density and turbidity currents. II Uniform flow of density currents. Can. J. Earth Sci., 3, pp. 627-637.

———1966c. Small-scale models of turbidity currents and the criterion for auto-suspension. J. Sediment. Petrol., 36, pp. 202-208.

———1967. Experiments on density and turbidity currents. III Deposition of sediment. Can. J. Earth Sci., 4, pp. 475-505.

MOIOLA, J., CLARKE, T., and PHILIPS, J. 1969. A rapid field method for making peels of unconsolidated sands. Bull. Geol. Soc. Amer., 80, pp. 1385-1386.

NESTEROFF, W. D. 1965. Le problème des turbidites; les données océanographiques modernes. Soc. Géol. Fr. Bull. Sér. 7, 7, pp. 587-592.

NORDIN, C. F., Jr., and BEVERAGE, J. P. 1965. Sediment transport in the Rio Grande, New Mexico. In Sediment transport in alluvial channels. U.S. Geol. Surv., Prof. Papers 462-F, p. 35.

OTTMAN, F. 1965. Introduction à la géologie marine et littorale. Masson, Paris, p. 259.

PARK, W. C. and AMSTUTZ, G. C. 1968. Primary 'cut-and-fill' channels and gravitational diagenetic features. Mineral. Deposita (Berl.), 3, pp. 66-80.

PETTIJOHN, F. J. 1957. Sedimentary rocks, 2 ed., Harper, New York, p. 718.

RICHARDSON, S. W., GILBERT, M. C. and BELL, P. M. 1969. Experimental determination of kyanite-andalusite and andalusite-sillimanite equilibria; The aluminum silicate triple point. Am. Jour. Sci., 267, pp. 259-272.

SANDER, B. 1970. An introduction to the study of fabrics of geological bodies. Pergamon Press; London, Toronto, p. 641.

SCHNEIDER, H.-J. 1964. Facies differentiation and controlling factors for the depositional lead-zinc concentration in the Ladinian Geosyncline. In developments in sedimentology, 2 (G.C. Amstutz, Ed.). Elsevier, Amsterdam, pp. 29-45.

SCHULZ, O. 1964. Lead-zinc deposits in the calcareous Alps as an example of submarine-hydrothermal formation of mineral deposits. In Developments in sedimentology, 2 (G.C. Amstutz, Ed.). Elsevier, Amsterdam, pp. 47-52.

SCOTT, S. D. and BARNES, H. L. 1971. Sphalerite geothermometry and geobarometry. Econ. Geol., 66, pp. 653-669.

SHEPARD, F. P. 1965. Importance of submarine valleys in funneling sediments to the deep sea. In Progress in Oceanography, 3 (M. Sears, Ed.). Pergamon Press, Oxford, New York, pp. 321-332.

SKINNER, B. J. 1958. The geology and metamorphism of the Nairne pyritic formation, a sedimentary sulfide deposit in South Australia. Econ. Geol., 53, pp. 546-562.

STONG, C. L. 1963. How to construct a stream table to simulate geological processes. Scientific Amer., 208, pp. 168-179.

THOMSON, B. P. 1965. Geology and mineralization of South Australia. In Geology of Australian ore deposits. Eight Commonwealth Mining and Metallurgical Congress, Australia and New Zealand, pp. 270-284.

van ANDEL, Tj. H. and KOMAR, P. D. 1969. Ponded sediments of the Mid-Atlantic Ridge between 22° and 23° North Latitude. Bull. Geol. Soc. Amer., 80, pp. 1163-1190.

WALKER, H. M. and LEV, J. 1969. Elementary statistical methods, 3 ed., Holt, Rinehart and Winston, New York, p. 432.

WALKER, R. G. 1970. Review of the geometry and facies organisation of turbidites and turbidite-bearing basins. In Flysch sedimentology in North America (J. Lajoie, Ed.). Geol. Assoc. Canada special paper no. 7, Toronto, pp. 219-251.

WHYTE, R. J. and GREEN, M. E. 1971. Geology and palaeogeography of Chibuluma West orebody, Zambian copperbelt. Econ. Geol., 66, pp. 400-424.